ADVANCED MATERIALS
www.advmat.de

Design Strategies and Applications of Dimensional Optical Field Manipulation Based on Metasurfaces

Wenwei Liu, Zhancheng Li, Muhammad Afnan Ansari, Hua Cheng, Jianguo Tian, Xianzhong Chen,* and Shuqi Chen**

Recent rapid progress in metasurfaces is underpinned by the physics of local and nonlocal resonances and the modes coupling among them, leading to tremendous applications such as optical switching, information transmission, and sensing. In this review paper, an overview of the recent advances in a broad range of dimensional optical field manipulation based on metasurfaces categorized into different classes based on design strategies is provided. This review starts from the near-field optical resonances of artificial nanostructures and discusses the far-field optical wave manipulation based on fundamental mechanisms such as mode generation and mode coupling. The recent advances in optical field manipulation based on metasurfaces in different optical dimensions such as phase and polarization are summarized, and newly-developed dimensions such as the orbital angular momentum and the coherence dimensions resulting from phase modulation are discussed. Then, the recent achievements of multiplexing and multifunctional metasurfaces empowered by multidimensional optical field manipulation for optical information transmission and integrated applications are reviewed. Finally, the paper concludes with a few perspectives on emerging trends, possible directions, and existing challenges in this fast-developing field.

1. Introduction

With the development of micro- and nanofabrication technologies, the exploitation of subwavelength localization of light has gathered burgeoning interest in the scientific community due to the versatile physical effects and revolutionary applications in photonics and quantum optics. Such localization of electromagnetic (EM) waves accompanies strong light-matter interactions and boosts the investigation of optical metamaterials and metasurfaces, which consist of arrays of artificial subwavelength building blocks that enable optical manipulation with high degrees of freedom. For example, numerous exotic optical effects and functionalities have been proposed based on the plasmonic electric and magnetic resonances induced by metallic meta-atoms, such as generalized laws of reflection and refraction,[1] negative permeability and permittivity,[2] photonic spin Hall effect,[3] cloaking,[4] and chirality.[5,6] In recent years, inspired by the multipolar Mie-type resonances in all-dielectric nanostructures, researchers have designed and developed more and more high-efficient functional devices. Compared with the metallic-based nanostructures, dielectric building blocks with high refractive indices do not suffer from intrinsic thermal loss, which leads to efficient designs with versatile functions, such as metalenses,[7–9] giant asymmetric transmission and chirality,[10,11] holography,[12–14] and special beams generation.[15]

On the other hand, mode coupling and mode superposition occurring in nanostructures inspire more optical effects and enable elaborate tailoring of optical properties.[16] For example, with simultaneous generation of electric and magnetic dipole resonances, split dielectric resonators can be used to realize an efficient Huygens' metasurface,[17] in which the Kerker effect occurs and the intensity of backward and forward scattering can be modulated through modes superposition when tailoring the geometric parameters of the nanostructures.[18] Strong coupling between the optical resonant modes can also be generated when the coupling criterion is satisfied. One of the most intriguing effects induced by the strong coupling is the bound states in the continuum (BICs), which theoretically have infinite state lifetime and ultra-high Q factors.[19,20] With the coupling between leaky resonances and guided modes, photonic BICs are actually vortex centers or polarization singularities in the momentum space.[21] Recently, based on the topological polarization singularities of symmetry-protected and accidental BICs,[22,23] researchers have developed more and more

W. Liu, Z. Li, H. Cheng, J. Tian, S. Chen
The Key Laboratory of Weak Light Nonlinear Photonics, Ministry of Education, Smart Sensing Interdisciplinary Science Center, Renewable Energy Conversion and Storage Center, School of Physics and TEDA Institute of Applied Physics
Nankai University
Tianjin 300071, China
E-mail: hcheng@nankai.edu.cn; schen@nankai.edu.cn
M. A. Ansari, X. Chen
School of Engineering and Physical Sciences
Heriot-Watt University
Edinburgh EH14 4AS, UK
E-mail: x.chen@hw.ac.uk
S. Chen
The Collaborative Innovation Center of Extreme Optics
Shanxi University
Taiyuan, Shanxi 030006, China

The ORCID identification number(s) for the author(s) of this article can be found under https://doi.org/10.1002/adma.202208884

DOI: 10.1002/adma.202208884

fascinating optical effects such as merging BICs,[24,25] topological protected charges when varying the geometric parameters,[19] generation and annihilation of BICs,[26] chiral BICs generation,[27,28] parity-time symmetry-induced BIC,[29] and enhanced nonlinear generation.[30,31]

The abundant optical resonances and mode interactions supported by the optical nanostructures further enable the multidimensional manipulation of optical waves from near field to far field.[32–34] Although most of the metasurfaces are based on resonant optics, some intriguing effects are free from resonances such as the Pancharatnam–Berry (P–B) phase,[35,36] which is induced from the symmetry of the optical building blocks, and the phase value is linearly determined by the orientation angle of the nanostructure. Taking advantage of the anisotropic designs of the building blocks, simultaneous and independent phase control under different polarization states has been realized based on metasurfaces,[37,38] which have been applied in polarized holographic multiplexing and polarization-controlled superposition of orbital angular momentum (OAM) states.[39–41] Simultaneous intensity and phase manipulation of optical waves can be employed to accurately control the energy ratio of each optical information channel and suppress the intrinsic noises in both linear and nonlinear regimes.[42,43] By combining different optical dimensions together, such as amplitude, phase, and polarization, researchers have also developed various multi-functional designs such as metasurfaces for full-space control of EM waves,[44] spin-selective chiral mirrors,[45,46] and waveguide-integrated metasurfaces.[47] Recently, the rapid development of metasurfaces has offered a profound perspective on photonics for integrated and functional devices that are challenging to be realized in conventional optics.

In this review article, we present an overview of the state-of-art technology across the rapidly developing research field of multifunctional metasurfaces for dimensional optical wave manipulation. We highlight the newly developed and combined optical degrees of freedom that underpin the profound progress in photonics in the past decade. We hope this review may serve the metasurfaces and photonics community as a catalyst for the future development of more and more fascinating optical effects and applications. The paper is structured as follows. In Section 2, we start from the basic principles of optical field manipulation in different optical dimensions, including the fundamental resonances to realize functional optical manipulation in different optical dimensions and the construction strategy of optical dimensions. Section 3 is dedicated to phase-based optical manipulation, including the P-B phase, resonance phase for wave-front control, and other optical dimensions induced from the phase such as OAM and coherence. Section 4 discusses recent advances in multidimensional metasurfaces empowered by polarization-based and customized optical manipulation. Dispersions and frequency-dependent optical manipulation are presented in Section 5, where we introduce the characteristic designs and applications operating in different frequency channels. Section 6 discusses optical manipulation in the momentum space, where optical functions are allocated to different directions. Finally, Section 7 offers an overview of several fascinating research fields that may provide other novel directions for optical field manipulation with metasurfaces.

2. Fundamentals and Principles: Resonances, Arrays, and Optical Dimensions

Generally, metasurfaces are based on resonant photonics, which enables light confinement at the sub-wavelength or even at the deep sub-wavelength scale. As a result, the optical properties of resonators, such as the lifetime of the states, dispersion, energy band, and scattering directivity rely highly on the geometric parameters of the resonators. For example, Yu et al. have demonstrated different phase abrupt by varying the shape of plasmonic antennas, which directly corresponds to the generated near-field resonant mode.[1] Considering the ubiquitous relations between the geometry and resonant mode of a resonator, abundant optical resonances occur for various geometric configurations and compositional materials.[10–12] On the other hand, the spatial setup of resonator arrays including in-plane, symmetric, and few-layer arrangement also provides a wide platform for mode generation and superposition.[13,16] Based on the geometry and resonance tailoring of the nanostructures, one can realize various optical functions in different optical dimensions such as phase, polarization, time, momentum, and frequency, as illustrated in **Figure 1**. Generally, optical resonances can be categorized into local and nonlocal resonances.

2.1. Local Resonances Generated by Nanostructures

The local optical resonances imply light-matter interactions confined in individuals or between adjacent nanostructures, which is one of the most exciting properties of nanophotonics with extreme light confinement. Based on the collective movement of electric charges, researchers have developed various types of local resonances in plasmonic metasurfaces such as electric dipoles (ED)[48] and magnetic dipoles (MD)[49] within different building blocks. In comparison, dielectric nanostructures can generate both electric- and magnetic-type resonances with comparable strengths, known as Mie scattering. The simultaneous generation of electric and magnetic multipolar resonances by dielectric resonators has boosted the research field of "Mie-tronics,"[50] which provides a profound impact on nanophotonics due to the lack of intrinsic thermal loss. Based on the abundant local resonances of nanostructures, recent advances in metasurfaces have presented versatile applications such as metalenses,[8] holography,[13] and spin-controlled wave-front shaping.[51] Furthermore, the scattering intensity and directivity of light can be modulated through the multipolar superposition of the existing modes through the Kerker effect.[18] The scattering intensity can be expressed as:

$$I = \frac{2\omega^4}{3c^2}|P|^2 + \frac{2\omega^4}{3c^2}|M|^2 + \frac{4\omega^5}{3c^4}(P\cdot T) + \frac{2\omega^6}{3c^5}|T|^2 + \frac{\omega^6}{5c^5}\sum\left|Q_{\alpha\beta}\right|^2 + \frac{\omega^6}{40c^5}\sum\left|M_{\alpha\beta}\right|^2 + \cdots \quad (1)$$

where P, M, T, $Q_{\alpha\beta}$, and $M_{\alpha\beta}$ are denoted as the ED, MD, toroidal dipole, electric quadrupole, and magnetic quadrupole, respectively. For instance, Yang et al. realized the simultaneous generation of multipole resonances in SiO_2-TiO_2-Si_3N_4 layered nanostructures, in which the mode interactions can be subtly

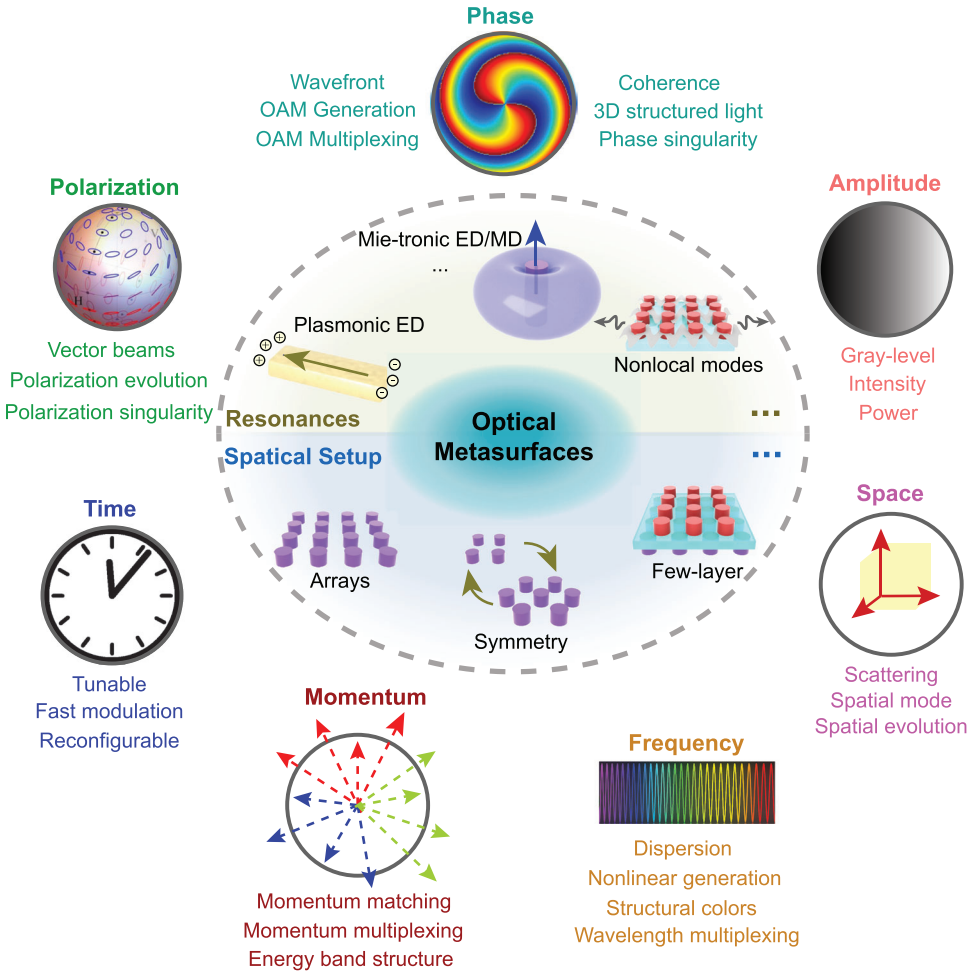

Figure 1. Schematic and principles for dimensional optical field manipulation with metasurfaces. Optical nanostructures with artificially tailored geometry can support abundant electromagnetic local and nonlocal resonances, such as the electric dipole (ED) and magnetic dipole (MD). With further spatial arrangement and symmetric engineering, metasurfaces enable versatile dimensional optical field manipulation from the development of fundamental photonics to applications of multi-functions integration and optical information transfer.

modulated by controlling the thickness of each layer.[52] The nanostructure can be regarded as a low Q-factor Fabry-Pérot resonator that suppresses optical scattering in low-frequency bands compared with pure titanium dioxide resonators.

To overcome the limiting Q-factors of subwavelength resonators, strong mode coupling can be introduced in the parametric space and realize avoided resonance crossing of frequency curves.[30] Different from the conventional BICs in arrays of nanostructures, Koshelev et al. realized a BIC mode in a subwavelength dielectric resonator and further boosted the second-harmonic generation efficiency. Such an effect originates from the mutual interference of several Mie-type modes and the quasi-BIC mode is achieved through the induced super cavity mode.[16] The mode coupling can be described by using a model of two coupled driven oscillators:[53,54]

$$\begin{pmatrix} \omega_1 - \omega - i\gamma_1 & g \\ g & \omega_2 - \omega - i\gamma_2 \end{pmatrix} \begin{pmatrix} x_1 \\ x_2 \end{pmatrix} = i \begin{pmatrix} f_1 \\ f_2 \end{pmatrix} \quad (2)$$

where $[x_1, x_2]^T$, $[\omega_1, \omega_2]^T$, $[\gamma_1, \gamma_2]^T$, $[f_1, f_2]^T$, and g are the oscillator amplitudes, resonant frequencies, damping coefficients, external force with driving frequency of ω, and coupling constant of the coupling system, respectively. The coupling between different resonances has provided more possibilities for optical manipulation with novel effects.

2.2. Nonlocal Resonances Generated by Artificial Arrays

The mechanism introduced in Equation (2) can describe any mode coupling system and of course applicable to nonlocal resonances. Unlike local optical resonances, nonlocal resonances originate from the global effects of the artificial arrays, such as the symmetry of the arrangement of nanostructures and leaky modes interactions between nanostructures. One type of nonlocal resonances is the so-called guided mode inside the arrays of periodic nanostructures. For example, a pair of leaky guided modesin periodic structured arrays strongly coupled with each other in momentum space, which further induces constructive

interference and destructive interference, leading to a low-Q radiative mode and a high-Q BIC mode, respectively.[55] Deng et al. investigated the coupling between the localized modes and guided modes, and an extreme degree of control over different diffraction orders was achieved with a giant dispersion.[56] Recently, Yang et al. realized significant improvement in third harmonic generation based on magnetic resonances induced BIC mode,[57] which efficiently suppresses the far-field fundamental radiation due to its high-Q factor nature.[58,59] Compared with the conventional designs with local resonances, the guided mode can also be employed to improve the Q factor of metasurfaces within an ultra-thin surface.[60–62] It should be noted that the nonlocal resonances are not limited to guided modes. As suggested in ref. [63], local resonances, adjacent interactions, or even long-range modes may exist in aperiodic arrays of nanostructures, especially in topologically optimized metasurfaces. Until now, how to combine and analyze different types of optical resonances and realize unexploited effects remain a challenge in current studies of metasurfaces.

2.3. Optical Manipulation in Multidimensions

Based on different types of optical resonances, one can realize dimensional manipulation of optical fields with metasurfaces. In the past decade, researchers have developed different schemes to control the intensity, phase, polarization, frequency, directivity, and their combination for optical engineering.[64–69] Generally, optical field manipulation in different dimensions can be categorized into two types. One is based on the non-orthogonal basis and the most commonly used ones are amplitude and phase. One can continuously modulate the scattering phase of a metasurface, and different values of phase are not orthogonal. Recently, researchers have developed spatial coherence as another optical dimension manipulated through metasurfaces,[70] which also leads to a non-orthogonal system. Another type of optical manipulation is based on the orthogonal basis. For example, any polarization can be realized through a linear combination of the orthogonal spin set $\{\sigma, -\sigma\}$. Another famous example is that optical information can be encoded in different directions, that is, at different locations inmomentum space. In Fourier optics, the basis functions $\{e^{ik_1x}, e^{ik_2x}, e^{ik_3x}, \ldots\}$form an orthogonal basis set, and each channel can be strictly distinguished from others, where k_1, k_2, and k_3 ... are the different momentum values normalized with the Planck constant. Since the momentum space describes exactly the spatial translational symmetry, it is widely used in energy band theory[20–22] and information multiplexing.[64] Similar properties are possessed by the frequency dimension with a basis set of $\{e^{i\omega_1 t}, e^{i\omega_2 t}, e^{i\omega_3 t}, \ldots\}$. Due to the orthogonal nature of different optical momentum or frequency components, one can feasibly obtain every component through a simple optical setup such as using a pinhole, a filter, or a 4f system. The momentum space has been applied to carry different metasurface-based information channels.[71,84] Similarly, one can also employ vortex beams as optical information channels because the basis functions $\{e^{il_1\theta}, e^{il_2\theta}, e^{il_3\theta}, \ldots\}$also form an orthogonal basis set, where l_1, l_2, and l_3 are different topological charges of each channel. Recently, researchers have proposed different strategies to realize parallel optical information transmission in multidimensions based on the abovementioned types of optical engineering. For example, Ouyang et al. achieved 6D optical information multiplexing by combining wavelength, polarization, and three spatial dimensions.[72] In the following sections, we will provide a detailed discussion of optical field manipulation in multidimensions.

3. Optical Manipulation in Phase-Based Multidimensions

Compared with electron-based information transmission, optical information transmission can carry parallel and concurrent tasks dut to the boson nature of photons, which are more difficult to be localized. Such non-locality is crucially affected by the phase and phase superposition of optical fields. Conventionally, optical phase is decided by the phase accumulation when light transmits inside the bulky medium. Taking advantage of the local resonances of nanostructures, metasurfaces can realize abrupt phase changes at the subwavelength scale. For example, by generating the local circuit resonances, the abrupt phase shifts can be achieved from 0 to 2π, which can be further employed to realize metalenses and OAM generation.[1,73] P-B phase is another famous one resulting from the relation among polarization conversion, incident helicity, and the orientation angle of nanostructures.[32] P-B phase can realize continuous phase modulation just by controlling the orientation of the nanostructures without modifying their geometric parameters. When considering nonzero-order diffraction components, the optical phase called the detour phase can also be continuously manipulated for continuous spatial movement of the nanostructures, which is a direct consequence of the diffraction effect on a discontinuous surface.[74]

3.1. Phase-Based Multi-Wave-Front Manipulation

Although theoretically, a local phase control from 0 to 2π is sufficient to realize optical focusing, however, it is much more complicated for practical applications. Generally, a lens suffers from different monochromatic aberrations and wavelength dispersions. Resembling the conventional lens design, the monochromatic aberrations can be corrected by applying a doublet corrected metasurface,[75,76] and the angle-of-view can be increased to 60°. The two metasurfaces located on both sides of the substrate append different wave-fronts to the optical waves, and the unfocused components can be fixed by the doublet metasurface. Another method to correct the monochromatic aberrations is proposed based on single-layer metalens arrays empowered by the machine learning technique.[77] Different sub-metalenses suffer from different aberrations, which can be combined together to remove the aberrations using a post-processing algorithm.

The wavelength dispersions of metalens can also be compensated by adding an additional wave-front onto the optical waves. When expanding the position and wavelength–dependent phase function using the Taylor series near the design frequency, one can obtain different orders of dispersion such as the relative group delay (first order) and group delay dispersion (second order).[78] Independent control of phase and dispersion

can be realized using coupled phase-shift elements with two nanofins in close proximity. By using polarization-insensitive building blocks, Wang et al. proposed a high-efficiency broadband achromatic metalens operating under arbitrarily polarized incidence,[79] as shown in **Figure 2**a. Figure 2b shows the required and theoretical group delay for broadband achromatism, which is achieved by the record-high aspect ratios of the nanostructures with near vertical sidewalls. The focusing properties in Figure 2c show significant achromatic focusing and can be applied in near-IR biological imaging. Generally, multi-wave-front manipulation can be realized by combining different types of optical phases such as P-B phase and resonance phase.[80] Recently, Song et al. realized a plasmonic topological metasurface, in which the building blocks are carefully designed to obtain a singularity in the scattering space (Figure 2d).[81] By analyzing the eigenfunctions of the scattering matrix, the eigenvalues and eigenstates degenerate at the operating wavelength of 600 nm, demonstrating the existence of exceptional point (EP), as shown in Figure 2e,f. Such development of phase control of optical waves based on subwavelength resonators has boosted the investigation and applications of multi-wave-front manipulation of metasurfaces.

3.2. Other Optical Dimensions Realized by Phase

As discussed in Section 2.3, other optical dimensions can also be constructed based on the optical phase. One of the most fascinating examples is the wave-front control using OAM as the information channel. As shown in Figure 2g, Ren et al. proposed an intriguing strategy for optical holography.[82] The optical information is encoded in different OAM channels which are mathematically orthogonal with each other, leading to a new OAM holography by utilizing strong OAM selectivity. The imaging information is bound with the OAM mode (Figure 2h). The same group also realized an OAM holographic technology with complex-amplitude modulation, and the multiplexing up to 200 independent (orthogonal) OAM channels were demonstrated.[83] Such technology also allows lens-less reconstruction and holographic videos for display and entertainment.

Another optical dimension induced by phase is spatial coherence. As shown in Figure 2i, by incorporating different disordered phase distributions characterized by the phase fluctuation range (PFR), the spatial coherence can be continuously controlled from fully coherent to nearly incoherent (Figure 2j).[70] The speckles shown in Figure 2k indicate lowered spatial coherence of the beams, in which smaller speckles corresponds to lower spatial coherence. The design strategy can be readily expanded to phase-only special beams such as vortex beams without refabricating the metasurface, and the modulated spatial coherence remains the same as the original Gaussian–Shell beam, as shown in Figure 2l. The optical fields with lowered spatial coherence can be applied in optical information transmission, and can be used to suppress the holographic artifacts.[85]

3.3. Nonlinear Phase-Based Optical Manipulation

The abovementioned phase modulation scheme can also be expanded in the nonlinear regime when considering the nonlinear resonances of the nanostructures. As shown in Figure 2m, the nonlinear generation highly depends on the symmetry of the nanostructures.[86] Similar to the selection rule in conventional nonlinear crystals, in which the locally generated nonlinear signals cancel when a certain symmetric lattice is adopted, nonlinear generation in metasurfaces can also be analyzed with local destructive or constructive superposition. Li et al. systematically investigated the relationship between the nonlinear P-B phase and the symmetry of the nanostructures.[87] It turns out that the value of the P-B phase is linearly decided by the order of the harmonic generation. These results provide intriguing schemes for nonlinear wave-front modulation with metasurfaces that can artificially control the order of harmonic generation by tailoring the symmetry of the nanostructures. Besides the nonlinear P-B phase, one can also realize nonlinear wave-front control by adopting the resonance phase. For example, Schlickriede et al. proposed an all-dielectric metalens that can achieve imaging of the third harmonic signals.[88] The nonlinear phase is locally modulated by controlling the diameters of the nanopillars. Basically, the nonlinear wave-front can also be manipulated based on the nonlocal resonances of the nanostructure arrays as introduced in the linear regime in ref. [62]. However, since the wavelength of nonlinear signals is much shorter than the fundamental signals, mode crosstalk or leakage raise a challenge to realize efficient wave-front control in an arbitrary channel.

4. Optical Manipulation in Polarization-Based Multidimensions

With the ongoing development of metasurfaces, optical field manipulation has progressed from the limited degrees of freedom at the beginning to polarization-based multidimensional manipulation. For example, the light was considered as a scalar field in the traditional holography with only two dimensions, that is, intensity and phase.[89] The polarization information was entirely overlooked in traditional holography, which has now demonstrated its significance in multi-channel and vectorial holography.[90–92] Thanks to their unprecedented capacities on simultaneous manipulation of amplitude, phase, and polarization state of optical waves at the subwavelength scale, meta-resonators with various sizes, geometries, and orientations are extensively exploited for polarization-dependent multidimensional manipulation.[93–97]

4.1. Orthogonal Polarization Multiplexing

Although polarization is equally essential among other attributes (i.e., phase and amplitude) of optical waves, it was omitted in the traditional diffraction optics and holography. The concept of polarization holography allowed the introduction of polarization information in bulky optics to a certain extent, which was used to demonstrate bi-channel holographic images under two orthogonal polarization states using traditional birefringent materials.[89,98] However, the potential of polarization-based multidimensional optical field manipulation, including the manipulation of both the spatial light field distribution and its polarization state distribution, cannot be entirely achieved due to the limited degrees of freedom in the conventional diffraction optics and the holographic recording medium.[90] As the immense progress has been made in the field of optical metasurfaces, many demonstrations have shown superior performances

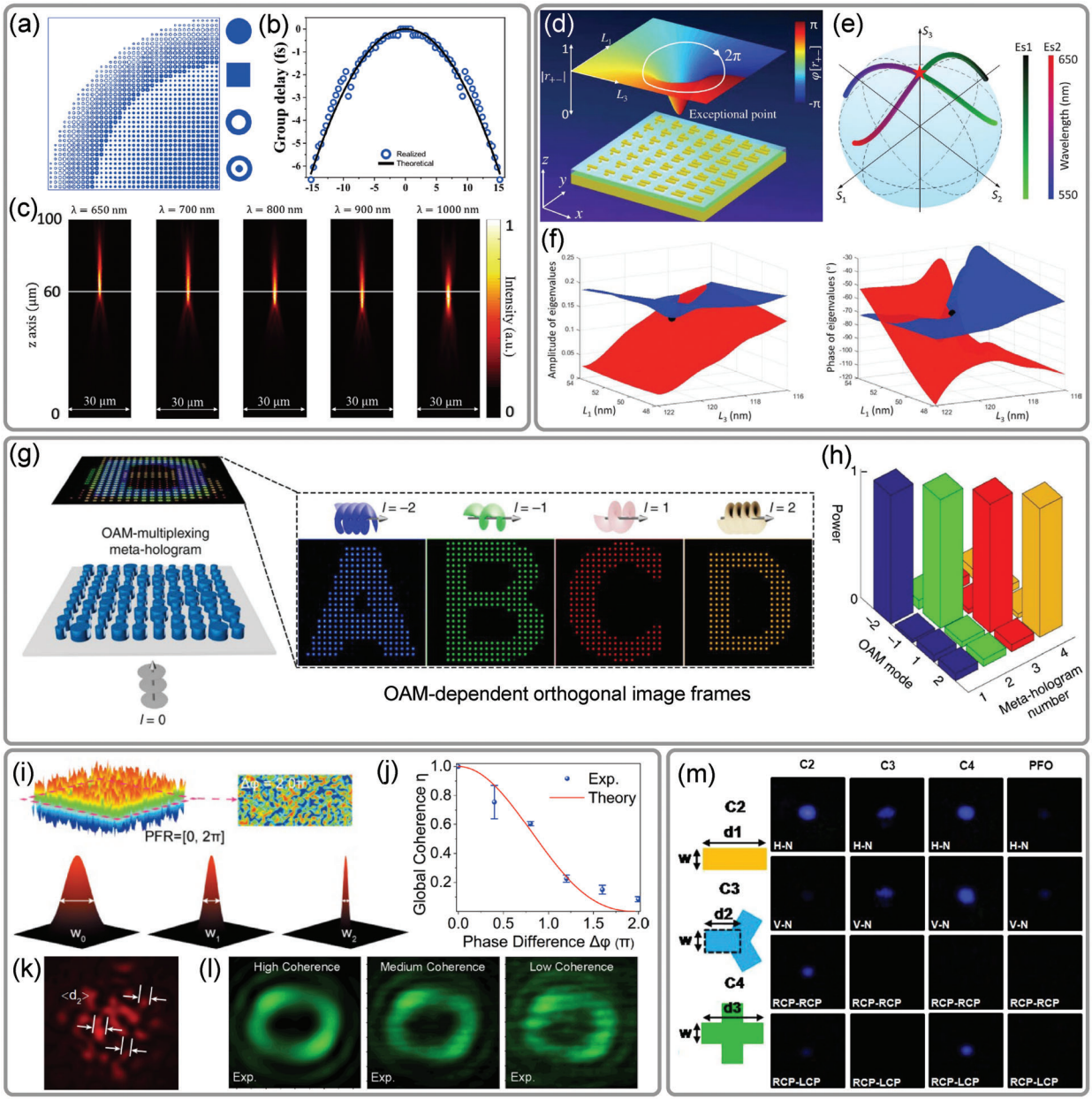

Figure 2. Optical manipulation and applications based on the phase domain. a–c) High-efficiency broadband and polarization-insensitive achromatic metalens for focusing and imaging operating in the near-IR biological imaging window. a) Geometric profiles of the titanium dioxide nanopillars with high vertical sidewalls for efficient optical phase manipulation. b) The required group delay for broadband achromatism and its realization with the nanopillars. c) Experimental focusing profiles operating at different wavelengths demonstrating the achromatic focusing property. d–f) Plasmonic phase manipulation by encircling an EP. d) Schematic of the EP-based phase manipulation by tailoring the geometric parameters of the nanostructures. e) Position of the eigenstates on the Poincaré sphere as a function of wavelength, and the degeneration occurs at 600 nm (red star). f) Simulated (left) amplitude and (right) phase of two eigenvalues at the operating wavelength of 600 nm, showing self-intersecting Riemann surfaces. g,h) Metasurface-based holography by utilizing strong orbital angular momentum selectivity. g) Schematic of an OAM-multiplexing meta-hologram, which realizes different image frames for different topological charges. h) The optical power of the reconstructed holographic images using different OAM beams, demonstrating the strong OAM selectivity. i–l) Coherence manipulation by incorporating a disorder-engineered wave-front of the metasurface. i) The spatial coherence can be manipulated either by controlling the PFR of the metasurface or by controlling the incident beam width. j) The global coherence can be manipulated from fully coherent to nearly incoherent. k) The instantaneous intensity distribution of speckles induced from the random distribution of the nanostructures and phase. l) The proposed coherence manipulation method can be expanded to other phase-only beams with the spatial coherence maintained. m) Nonlinear P-B phase decided by the symmetry of the resonators. For different symmetries of the nanostructures(left), the generated third harmonic generation is symmetry-selective, and some nonlinear channels are blocked depside the original symmetry of the material allowing for the nonlinear generation. Panels reproduced with permission from: a–c) Reproduced with permission.[79] Copyright 2021, Springer Nature. d–f) Reproduced with permission.[81] Copyright 2021, American Association for the Advancement of Science. g,h) Reproduced with permission.[82] Copyright 2019, Springer Nature. i–l) Reproduced with permission.[70] Copyright 2022, American Chemical Society. m) Reproduced with permission.[86] Copyright 2014, American Physical Society.

in the pursuit of multiple degrees of freedom in optical manipulation. Furthermore, based on such unique manipulation, multidimensional optical manipulation integrated into a single metasurface is achieved, particularly manifesting helicity multiplexing or orthogonal physical channel multiplexing such as polarization. Wen et al. demonstrated a helicity multiplexed metasurface hologram, as shown in **Figure 3**a.[99] In this work, two central symmetric and off-axis holographic images (flower and bee) were interchanged by changing the helicity of the circularly polarized light. The orthogonal polarization multiplexing for circularly polarized light was achieved by merging two sets of metasurfaces consisting of metallic nanorods. This approach helped solve various challenges associated with conventional computer-generated holograms, such as bandwidth, efficiency, and image quality. Orthogonal polarization multiplexed metasurfaces sensitive to the linear or elliptical polarization of the incident light have also been investigated.[65,74] Unlike the helicity-multiplexed metasurface holograms, Min et al. reproduced and controlled two distinct wave-fronts using incident light with two orthogonal linear polarization states.[74] In this work, plasmonic nano-silts were employed to realize the arbitrary detour phase distribution with strong orthogonal and linear (*s* and *p*) polarization-dependent wave-fronts (Airy beam and optical vortex, respectively) at a broadband wavelength. Lately, concise design principles for independent phase and amplitude manipulation of optical waves with arbitrary orthogonal polarization states (circular, linear, or elliptical) have been proposed and well demonstrated.[38,65] The bi-channel multiplexing with two pairs of orthogonal polarization states has attracted exciting and pragmatic applications in optical field manipulation, that is, stimuli-responsive tunable metaoptics,[100] real–time biomedical and chemical substance detection for environmental monitoring and public health sector,[101] and dual-sided displays for AR-VR technology.[102] For example, a compact volatile gas sensor platform was experimentally demonstrated by combining liquid crystals with an asymmetric transmission-type metasurface[97,103,104] to rapidly sense the presence of isopropyl alcohol (IPA) gas in real-time with a visual holographic alarm state, as shown in Figure 3b.[101] Here, the gas responsiveness was investigated in different geometries of the liquid crystals (isotropic and nematic) with the asymmetric transmission-type metasurface relying on propagation and retardation phase. The overall retardation phase through the liquid crystal medium was controlled by the liquid crystal cell ordering. The change in the order of liquid crystal cells governs the change in the effective refractive index of the device. Consequently, the desired polarization state of the output beam from the asymmetric metasurface was adjusted by the tunable phase retardation of liquid crystal cells.

To further simplify the design complexities and manufactural challenges of multi-layer asymmetric structures, Ansari et al. presented a single-layer and relatively simple approach to realize a unique type of orthogonal polarization-based multidimensional functionality, that is, direction-multiplexed meta-holography as shown in Figure 3c.[102] The design is comprised of nano-featured half-wave plates carefully optimized to excite the antiferromagnetic resonance modes (antiparallel magnetic dipoles and induced electric displacement currents) to ensure the high transmission of converted components for the direction multiplexed multidimensional functionality. The assemblies of antiparallel magnetic diploes and alternate electric displacement currents under the illumination of *x* and *y*-polarized light are responsible for the desired phase delay (π) between output orthogonal electric field components, as shown in Figure 3c. However, the theoretical efficiency of such a design is limited to 50% due to the geometric phase modulation.[105] Therefore, a more efficient single–layer metasurface was proposed to demonstrate unique orthogonal polarization multidimensional manipulation, that is, simultaneous circular symmetry breaking and multi-channel wavefront shaping.[103,105] Unlike the previous design, in this work, asymmetric spin-orbit interactions (ASOIs) were used instead of symmetric spin-orbit interactions. A symmetry-breaking supercell design of dielectric resonators was employed to excite ASOIs with giant asymmetric transmission for bidirectional diffraction patterns (lens, vortex beam, and hologram), as shown in Figure 3d.[105] Recent progresses have further demonstrated that metasurfaces can not only be utilized to realize independent multidimensional manipulation of optical waves with orthogonal polarization states, but also be used to realize independent phase and amplitude manipulation of optical waves with non-orthogonal polarization states, which further expand the capacity of metasurfaces for optical polarization multiplexing.[106,107]

4.2. Discrete Polarization Distribution

Although the bi-channel orthogonal polarization multiplexing has provided a significant start for the polarization-based optical manipulation, the complete and simultaneous reproduction of coherent wave-fronts with desired multiple states of polarization and distributions is not realized until the advent of full vectorial metasurfaces. Therefore, a vectorial metasurface with more than two degrees of freedom is required to further increase the number of polarization channels and to construct multiple wavefronts with spatially varying distributions of polarization. The first vectorial metasurface was proposed by interleaving diatomic plasmonic resonators-based sub-units. Consequently, a particular polarization state is associated with each sub-unit of the vectorial metasurface, as shown in Figure 3e.[108] The diatomic meta-atoms are comprised of two similar and orthogonal plasmonic nanorods, which were subjected to detour and geometric phase modulations for independent control of polarization and wavefront. In this work, the extra degree of freedom originates from the relative local displacement between the orthogonal nanorods, the orientation angle, and the global displacement of the unit-element boundary.

Similarly, to further increase optical information channels in more optical dimensions, the tunable and discrete vectorial holography in combination with structural color printing was experimentally demonstrated for the advanced photonic encryption application using a pixelated metasurface as shown in Figure 3f.[14] The device can display a color QR code in the near-field and vectorial images in the far-field with discrete polarization states under the illumination of the white light and the coherent light, respectively. Here, the asymmetric nano-bars acting simultaneously as waveguides and Mie-resonators were utilized to independently control phase and reflection spectrum, respectively. Further integration of pixelated metasurface with liquid crystal has enabled electrical tunability for color printing with

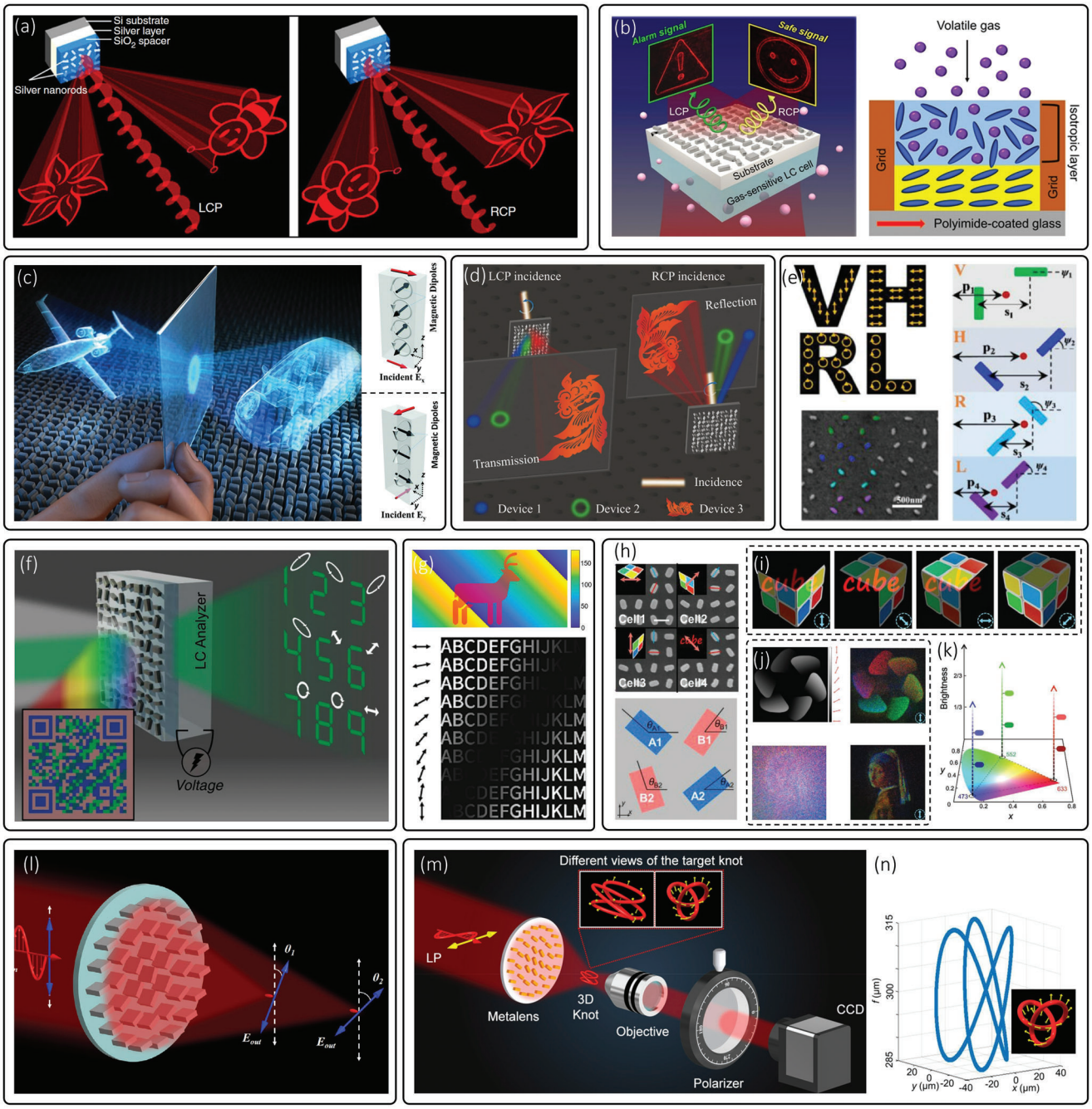

Figure 3. Optical manipulation in polarization-based domains. a) Helicity multiplexed metahologram producing flower and bee in the reflection domain under LCP and RCP illuminations. b) Left: Schematic of metasurface-based rapid gas sensor for visual alarm, which generates visual safe and alarm signs in the absence and presence of a dangerous volatile gas, respectively. Right: Schematic illustration of side view of a liquid crystal cells (elliptical shape) stimulated with volatile gas molecules (round shape). The order of liquid crystal is decreased because of the inclusion of gas molecules into the liquid crystal layer. c) Left: Conceptual diagram of direction-multiplexed metahologram operating in both forward and backward directions. Right: Dielectric antiferromagnetic resonance modes inside the optimized nanorod under *x*- and *y*-polarized illuminations. Red arrows show the direction of incident and output electric fields. Black arrows show the direction of antiparallel magnetic dipoles and white circular arrows show the direction of induced electric displacement currents inside the optimized nanorod. d) Schematic diagram of spin-selective wave-front shaping and giant asymmetric transmission through ASOIs. e) Single vectorial metasurface generating horizontally polarized, vertically polarized, LCP and RCP light using diatomic unit-cells with varying orientation, local, and global displacements. f) Illustration of pixelated metasurface integration with liquid crystal for dynamic vectorial holographic color printing. g) Top: Conceptual holographic image of a deer with continuous polarization distribution. Bottom: Obtained holographic patterns with varying angles of the analyzer. Holographic patterns from top to bottom correspond to the angle of analyzer changing from horizontal to vertical direction. h–k) Vectorial metasurfaces with kaleidoscopic polarization distribution. h) Four sub-cells with corresponding color images (shown in the insets) with tetratomic macro-pixel (shown in the bottom panel). i) Reproduced results of polarization-multiplexed kaleidoscopic holography with blue arrows depicting the angle of analyzer. j) Kaleidoscopic holographic display with continuous-polarization encryption. Right panel shows measured

vectorial holography. The research has opened new possibilities for high-quality photonic security and cryptographic devices.

4.3. Continuous and Kaleidoscopic Polarization Distribution

Since the number of interleaved sub-units is limited, the output field has a discrete distribution of polarization states with a finite number, as observed in the previous subsection. To overcome this limitation, a more general approach is required to encode an infinite number of polarization states for continuous vectorial field manipulation. One unique approach to realizing continuous vectorial distribution is by combining the same target phase map (for left and right circularly polarized (LCP and RCP) incident light) with a unique detour phase in x and y-directions.[109] The detour phase between two geometric metasurfaces with identical wavefronts ensures a continuous modulation of relative phase shift between LCP and RCP components. As a result, a continuously changing linear polarization loaded on a hologram was obtained as shown in Figure 3g. The continuously moving dark region upon changing the angle of the analyzer proves the concept of an infinite number of polarization states for continuous vectorial and multidimensional field manipulation. A few other demonstrations of continuous vectorial field manipulations were also realized using different modified iterative approaches.[110–112]

Later, researchers made efforts to further expand the spectral manipulation based on metasurfaces to full-color vectorial holography with designed polarization distributions.[113,114] Guo et al. used the k-space engineering and vector superposition through macro-pixels comprised of four meta-atoms, as shown in Figure 3h. Full-color holographic wave-fronts were loaded with well-designed (circular, elliptical, and linear) polarization channels using a complete control of azimuthal angle and ellipticity, as shown in Figure 3i. Furthermore, they realized the brightness tuning of kaleidoscopic holographic images by controlling the orientation of polarization (Figure 3j). The modulable colors were transformed from RGB color to a 3D hue, saturation, and brightness (HSB) color space, as illustrated in Figure 3k,j. Unlocking the brightness dimension in metasurface-based holography can significantly improve the chiaroscuro of full-color images by making them more vivid and realistic.[115]

4.4. Customized Multidimensional Polarization Fields

With further enhanced degrees of freedom enabled by metasurfaces, another unique type of polarization-based multidimensional field manipulation was proposed, which enables customized polarization distribution at any arbitrary focal position in 3D space.[116–118] Zang et al. presented multi-foci metalenses comprised of the well-defined polarization rotation directions at different focal planes under linearly polarized incident light, as shown in Figure 3l.[117] Furthermore, the longitudinal, and transversal multi-foci lensing with the engineered polarization rotation distribution were presented, leading to the generation of customized vectorial 3D focal curves as shown in Figure 3m. A metalens-based general approach was used to simultaneously manipulate the polarization distribution and intensity profile in real space for any arbitrary shape, that is, optical focal curves and 3D knots (Figure 3m,n).[116] The proposed work is a relatively simple and powerful approach for generating arbitrary polarization distributions of 3D optical fields and can find several exciting applications in particle manipulation and nanolithography.

5. Optical Manipulation in the Frequency-Dependent Dimension

Due to the incoherence between optical waves with different frequencies, the optical frequency has been becoming a very important degree of freedom for frequency-selective and multi-channel optical wave manipulation. Specifically, the optical resonances of metasurfaces can be precisely manipulated. Optical resonances with on-demand resonant frequency, bandwidth, and strength have been extensively realized in metasurfaces, which are widely used for the realization of vivid structural colors and frequency-selective optical wave manipulation.[33,119] Further, optical waves at different frequencies can be independently manipulated based on metasurfaces, providing high capabilities for the realization of optical multi-functional integration and multiplexing.

5.1. Frequency–Domain Optical Resonances

Manipulating the optical resonances of metasurfaces in the frequency domain is the foundation of frequency-dependent optical function integration and multiplexing. The resonant frequency, bandwidth, and strength of metasurfaces can be efficiently modulated by adjusting the structural parameters, resulting in efficient amplitude manipulation of optical waves in both single frequency and broad bandwidth. Optical amplitude manipulation at a fixed frequency has been well proposed in metasurfaces by employing three basic principles: adjusting the resonant strength at the interested frequency, shifting the resonant frequency, and utilizing the optical collective interference effect between different resonators.[65,120–124] It is remarkable that metasurfaces designed based on the optical collective interference effect provide simple and powerful candidates for continuous and arbitrary optical amplitude manipulation.[65,124] In addition, based on Malus's law, metasurfaces composed of anisotropic resonators

results with polarization analyzer and left bottom panel shows measured result without polarization analyzer. k) 3D hue, saturation, and brightness (HSB) color space. l–n) Customized 3D polarization fields using multi-foci meta-lensing approach producing l) well-defined polarization rotation on longitudinal and transversal directions, m) customized vectorial 3D arbitrary curves, and n) optical knots. Panels reproduced with permission from: a) Reproduced with permission.[99] Copyright 2015, Springer Nature. b) Reproduced with permission.[101] Copyright 2021, American Association for the Advancement of Science. c) Reproduced with permission.[12] Copyright 2018, Royal Society of Chemistry. d) Reproduced with permission.[105] Copyright 2017, Wiley-VCH. e) Reproduced with permission.[108] Copyright 2018, American Chemical Society. f) Reproduced with permission.[14] Copyright 2021, Springer Nature. g) Reproduced with permission.[109] Copyright 2021, American Chemical Society. h–k) Reproduced with permission.[113] Copyright 2022, Wiley-VCH. l) Reproduced with permission.[117] Copyright 2019, Wiley-VCH. m,n) Reproduced with permission.[116] Copyright 2021, American Chemical Society.

have been widely used to manipulate the optical amplitude at one or multiple fixed linear polarization directions.[125–127] Metasurfaces designed based on Malus's law can realize optical amplitude manipulation in a broad bandwidth and the operation bandwidth is mainly decided by the resonant bandwidth of the metasurfaces.[128] Due to the excellent capacity of metasurfaces on frequency-dependent optical amplitude manipulation at the subwavelength scale, they have been widely used for the realization of high-level gray imaging and optical encryption. Moreover, by modulating the optical resonances of metasurfaces in the entire visible spectrum, metasurfaces have been utilized to realize structural colors, which is one of the key applications of metasurfaces and shows an extensive value for advanced imaging and optical display.[119,129] Transmissive and reflective structural colors with different brightness, hue, and saturation values have been well demonstrated in both metallic and dielectric metasurfaces. In particular, dielectric metasurfaces are widely used for the implementation of structural colors with high brightness and saturation since their inherent loss is negligible in the visible regime.[130–132] There are two main approaches for the manipulation of optical resonances of dielectric metasurfaces in the frequency domain dimension to realize vivid structural colors: introducing new resonant manipulation mechanisms and improving the degree of structural design freedom.[52,133–137] For example, Yang et al. proposed multipolar-modulated metasurfaces composed of dielectric nanostructures with multiple stacked layers to significantly suppress the unwanted multipolar resonance modes away from the center frequency.[52] The index matching effect between the layers can dramatically enhance the monochromaticity of the reflection spectra, which results in structural colors with ultra-high saturation ranging from 70% to 90% with full hue. The other example is the realization of transmissive structural colors with different HSB values by fully manipulating the structural geometry of the nanopillar based on two-photon polymerization lithography method.[137] As shown in **Figure 4**a, the height and diameter of the nanopillar, and the distance between the nanopillars can be fully controlled in the fabrication, which provides a high degree of structural design freedom. As a result, the resonances of nanopillars can be effectively manipulated and the HSB values of transmissive structural colors can be efficiently modulated with a wide coverage of the full HSB color space as shown in Figure 4b,c.

Recent advances further prove that the control range of optical resonances of metasurfaces in the frequency domain can be further expanded by adding multiple nanostructures in one unit cell. Structural colors with arbitrary HSB values and the multi-color mixing can be implemented by utilizing polyatomic metasurfaces whose unit cell is composed of several nanostructures.[13,138,139] Moreover, the anisotropic optical resonances of asymmetric nanostructures provide an effective way to realize two different structural colors with apparent color contrast in one frequency channel, which has been widely used for optical encryption and anti-counterfeiting.[12,140,141] In these approaches, the unit cells in metasurfaces show two distinct structural colors under illuminations of two orthogonal polarization states. The HSB values of structural colors can be continuously modulated by changing the polarization state of the incident wave. This feature recently has been utilized to realize colorimetric polarization-angle detection based on deep-learning algorithms, as shown in Figure 4d.[142] A dual-color palette with arbitrary color combinations under linear orthogonal polarization states was obtained by using bilayer stacked nanopillars with different diameters and periods. Then a residual-network-based detection algorithm is trained to find the relationship between the color palette variation and the polarization angle of incident wave. The well-trained algorithm can accurately recognize extremely slight polarization variations, which significantly improves the compactness of polarization detection while maintaining high accuracy. This work demonstrates that metasurfaces' arrays with customized frequency-dependent optical resonances can be used for optical field detection with high accuracy and compactness. Recently, the advantage of deep-learning technology on multi-task optimization has also been used to realize optical manipulation in the frequency domain. Nanostructures with desired resonant frequency, bandwidth, and strength can be obtained based on well-trained deep-learning algorithms, providing an effective way for the realization of desired structural colors.[143,144]

5.2. Optical Multi-Functional Integration and Multiplexing in the Frequency-Dependent Dimension

Besides the manipulation of resonant frequency, bandwidth, and strength in the frequency-dependent dimension, the phase of scattering field can also be effectively manipulated based on metasurfaces. Recently, segmented and interleaved metasurfaces are widely used for optical multi-functional integration and multiplexing in the frequency-dependent dimension, in which different nanostructures in one unit cell or the same nanostructures in different area work at different operating frequencies.[64,145–150] For example, a segmented metallic metasurface composed of nanoapertures was proposed to realize the generation of focus OAM beams with different topological charges at two different wavelengths.[145] Multi-color meta-holography has been well demonstrated in metasurfaces by independently manipulating the phase of optical waves at the three distinct frequency channels correlated to the red, blue, and green colors. As shown in Figure 4e, an interleaved dielectric metasurface formed by three kinds of nanoblocks in one unit cell can realize the simultaneous phase manipulation for red, blue, and green optical waves, and multi-color meta-holograms were achieved.[148] The integration of multi-color nanoprinting and holography has also been implemented based on interleaved metasurfaces composed of diatomic nanostructures by simultaneously manipulating the amplitude and phase of optical waves at different operation frequencies.[13] Further, realizing polarization-selective optical manipulation in the frequency domain can significantly expand the optical functionalities of metasurfaces since the complex amplitude of optical waves at different operation frequencies can be independently manipulated under different polarization states.[149] Polarization-controlled color-tunable hologram was implemented based on an interleaved metasurface by independently manipulating the phase of optical waves at two different frequency channels in two orthogonal polarization states.[150] Anisotropic metasurfaces' design based on Malus's law has been demonstrated as good candidates for the integration of multi-color nanoprinting and holography.[151–153] For example, interleaved metasurfaces composed of dielectric nanobricks were proposed for tri-channel

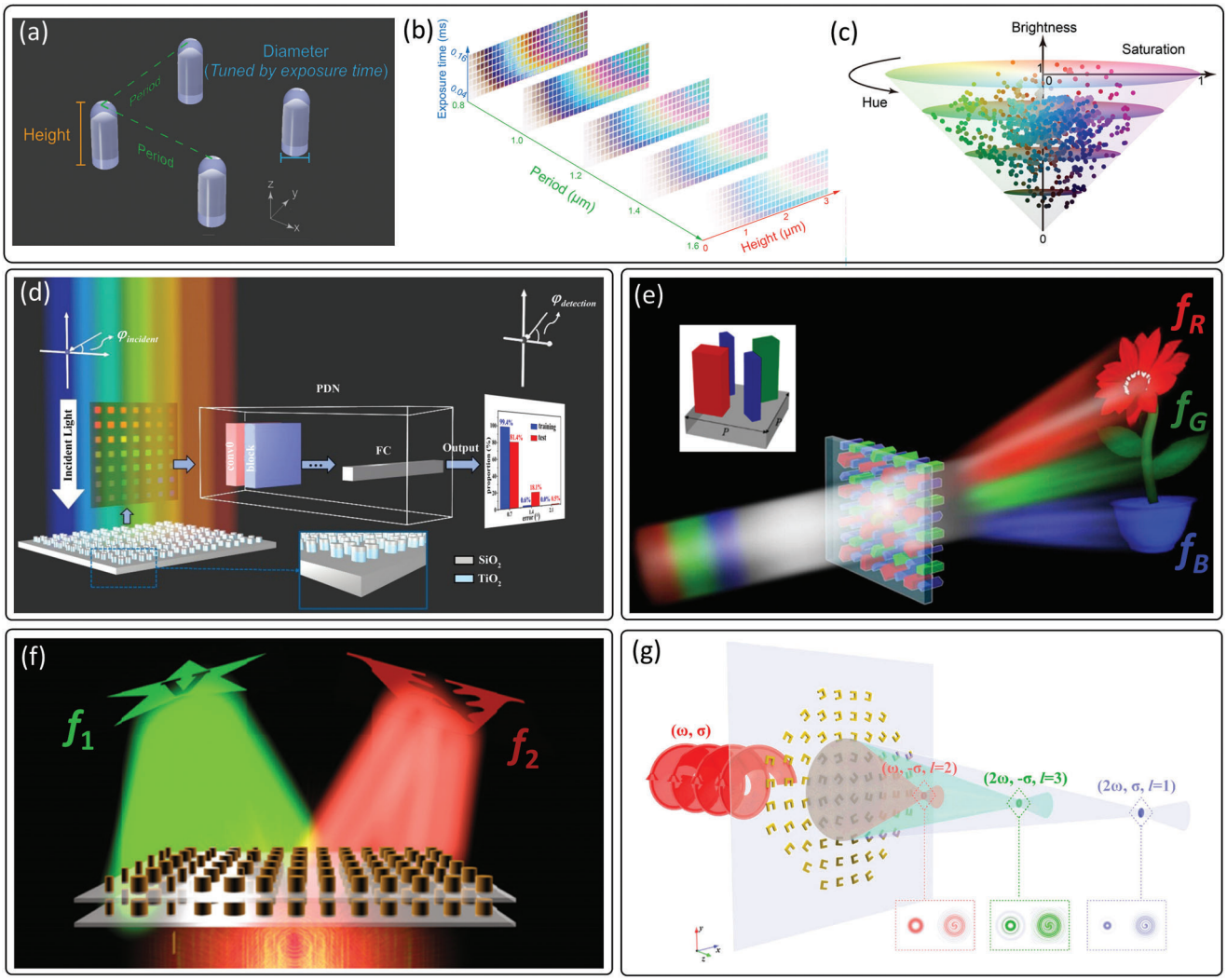

Figure 4. Optical manipulation in the frequency domain. a–c) Full color palette in 3D color space based on metasurfaces composed of nanopillars: a) Schematic of the nanopillar with three structural variables: the height and diameter of the nanopillar, and the period. b) The variation of the transmissive structural color of the nanopillar-based period metasurfaces with the changing of the three structural variables of the nanopillar. c) The corresponding 3D HSB color space from the results in (b). d) Schematic of colorimetric polarization-angle detection based on asymmetrical all-dielectric metasurfaces. e) Illustration of the multi-color holography based on an interleaved dielectric metasurface. Inset: Schematic of the basic unit cell composed of four Si nanoblocks working at three different frequency bands. f) Schematic of frequency selective meta-holography based on a bilayer dielectric metasurface. g) Illustration of a metallic nonlinear metasurface for the realization of focusing optical vortices at both the fundamental frequency and the second harmonic generation. Inset: Numerical intensities and interference patterns of the corresponding optical vortices. Panels reproduced with permission from: a–c) Reproduced with permission.[137] Copyright 2021, American Chemical Society. d) Reproduced with permission.[142] Copyright 2022, Optica. e) Reproduced with permission.[148] Copyright 2016, American Chemical Society. f) Reproduced with permission.[156] Copyright 2019, Springer Nature. g) Reproduced with permission.[162] Copyright 2018, Wiley-VCH.

near- and far-field polychromatic image displays.[153] Besides the segmented and interleaved metasurfaces, few-layer metasurface is another good alternative for the realization of multi-frequency optical integration and multiplexing.[154–156] For example, a bilayer dielectric metasurface was proposed to realize meta-holography in two frequency channels, as shown in Figure 4f.[156] The bilayer design can dramatically expand the degrees of structural design freedom of metasurfaces, and optical functionalities in different frequency channels can be independently implemented by different layers. By further combining the few-layer, segmented, and interleaved design strategies, the capacity of metasurface for optical manipulation can be considerably improved, empowering the realization of spin, frequency, and wavevector-dependent optical multi-functional integration.[157] Certainly, multi-frequency optical integration and multiplexing can also be realized by using common metasurfaces, in which every unit cell is composed of one nanostructure that can independently manipulate optical waves at multiple frequency channels. For example, complete independent phase manipulation at two frequencies was realized by varying two structural parameters of the unit cell in few-layer metasurfaces, in which the nanostructure in every unit cell consists of two resonators

working at the two operation frequencies respectively.[158] As another example, different 1-bit gray images can be observed at two frequency channels respectively for metasurfaces composed of four kinds of nanostructures.[45] The four nanostructures can be represented as the "00," "01," "10," and "11" intensity coding elements, which can realize independent reflective intensity manipulation at two different frequencies. However, the design and optimization of nanostructures that can simultaneously manipulate optical waves at different frequency channels is quite difficult. Deep-learning empowered inverse design method recently emerged as a powerful alternative to solve this problem.[159,160] Predictably, efficient optical manipulation with a high degree of freedom in the frequency-dependent dimension can be further implemented by inversely designed metasurfaces.

Moreover, multi-frequency optical integration and multiplexing can also be realized by using nonlinear metasurfaces that can simultaneously manipulate the fundamental waves and the corresponding harmonics.[39,40,161,162] For example, a nonlinear metasurface composed of metallic split ring resonators (SRRs) was proposed to realize one linear and two second harmonic optical focus vortices with different topological charges by introducing both the linear and nonlinear geometric phase as shown in Figure 4g.[161] For an SRR with a rotation angle θ along the wave propagation direction, the geometric phase of fundamental wave with an opposite handedness ($-\sigma$) of the circular polarization to that (σ) of the incident wave can be expressed as 2θ, while the nonlinear geometric phase of the second harmonics with the same or opposite circular polarization to that of the fundamental wave are θ and 3θ. Therefore, the wave-front of both fundamental waves and nonlinear harmonics can be manipulated simultaneously. By precisely controlling the rotation angles of nanostructures in nonlinear metasurfaces, multi-frequency meta-holography, and optical multiplexing were also realized.[39,40]

6. Optical Manipulation in the Momentum Space

In addition to the fact that optical waves with different k vectors can be used for multi-channel optical manipulation, optical field manipulation in the momentum space based on metasurfaces shows some distinct advantages when compared with the optical filed manipulation in other dimensions based on metasurfaces. For example, by adjusting the angular-dependent resonances of metasurfaces, the metasurfaces can show different optical functionalities under the illumination of optical waves with different k vectors. The switching between different functionalities can be simply implemented by changing the relative angle of metasurface to the k vector of incident wave. In addition, some metasurfaces whose optical responses are adjusted in an area of the k space are without real-space centers. This key feature lowers the requirement on center alignment of optical devices and benefits the optical integration.

6.1. Angular-Selective and -Multiplexed Optical Manipulation

Since the angular dispersion of resonances in metasurfaces can be manipulated, metasurfaces have become efficient alternatives for the implementation of angular-selective and -multiplexed manipulation of optical waves. By carefully controlling the radiation pattern of single metallic nanostructure and the near-field couplings between the metallic nanostructures, metasurfaces with desired angular dispersion have been well demonstrated.[163,164] **Figure 5**a presents an angle-multiplexed meta-polarizer designed by manipulating the angular dispersion of the metasurface. The optical resonances of the meta-polarizer under TE and TM illuminations with different incident angles can be purposely manipulated, and then the polarization state of the reflected wave can be controlled by changing the k vector of the incident wave, as shown in Figure 5b. By introducing the near-field couplings between the nanostructures, the k vector of the incident wave can also be the key variable that determines the resonance mode of the metasurface.[165] These approaches indicate that optical waves can be effectively manipulated in the momentum space by controlling the angular-dependent optical resonances of metasurfaces.

Meanwhile, angular-selective optical wave-front manipulation has been realized by controlling the optical phase shifts in metasurfaces. Figure 5c shows a gradient metasurface for the realization of angular-asymmetric optical absorption which is attributed to the angular-selective excitation of evanescent wave propagation along the surface.[166] The gradient metasurface provides a large phase gradient along the x-direction. For reflection coefficient R_1 equals to 0.99, the TE waves illuminated at an angle θ_i will be reflected backward while that illuminated at an angle $-\theta_i$ will be converted into evanescent waves resulting in the high absorptance as shown in Figure 5d. Moreover, angular-multiplexed meta-holography has also been realized based on metasurfaces, in which the optical phase shifts for different incident angles can be independently controlled.[71,167]

6.2. Optical Manipulation in an Area of the Momentum Space

Recent advances in metasurfaces further prove that the optical responses of metasurfaces can be manipulated not only at several fixed k vectors, but also in an area of the k-space. Optical analog computing has been realized by fully controlling the optical responses of metasurfaces in an area of k-space, which shows great application potential in image processing, edge detection, and machine learning.[168] For example, optical image differentiation can be realized in metasurfaces with carefully designed transfer function $T(k_x, k_y)$.[169,170] Figure 5e shows the basic unit cell of a polarization-insensitive metasurface for the implementation of second-order differentiation on optical images, for which $T(k_x, k_y) = -A(k_{||})^2$ and A is a constant. Such $T(k_x, k_y)$ was realized by using the strong nonlocality of Fano resonance manifesting as the shift of resonant wavelength versus incident angle, as shown in Figure 5f. As a result, the polarization-insensitive metasurface can realize efficient 2D edge detection with numerical aperture NA = 0.1392 as shown in Figure 5g. By manipulating the optical responses of metasurfaces in the k-space, metasurfaces can be further utilized to realize some special optical devices, such as optical spaceplate.[171] Since optical devices with larger NAs are preferred in real applications, therefore, the realization of optical manipulation in a large area of k-space (with a high NA) still needs to be further investigated.

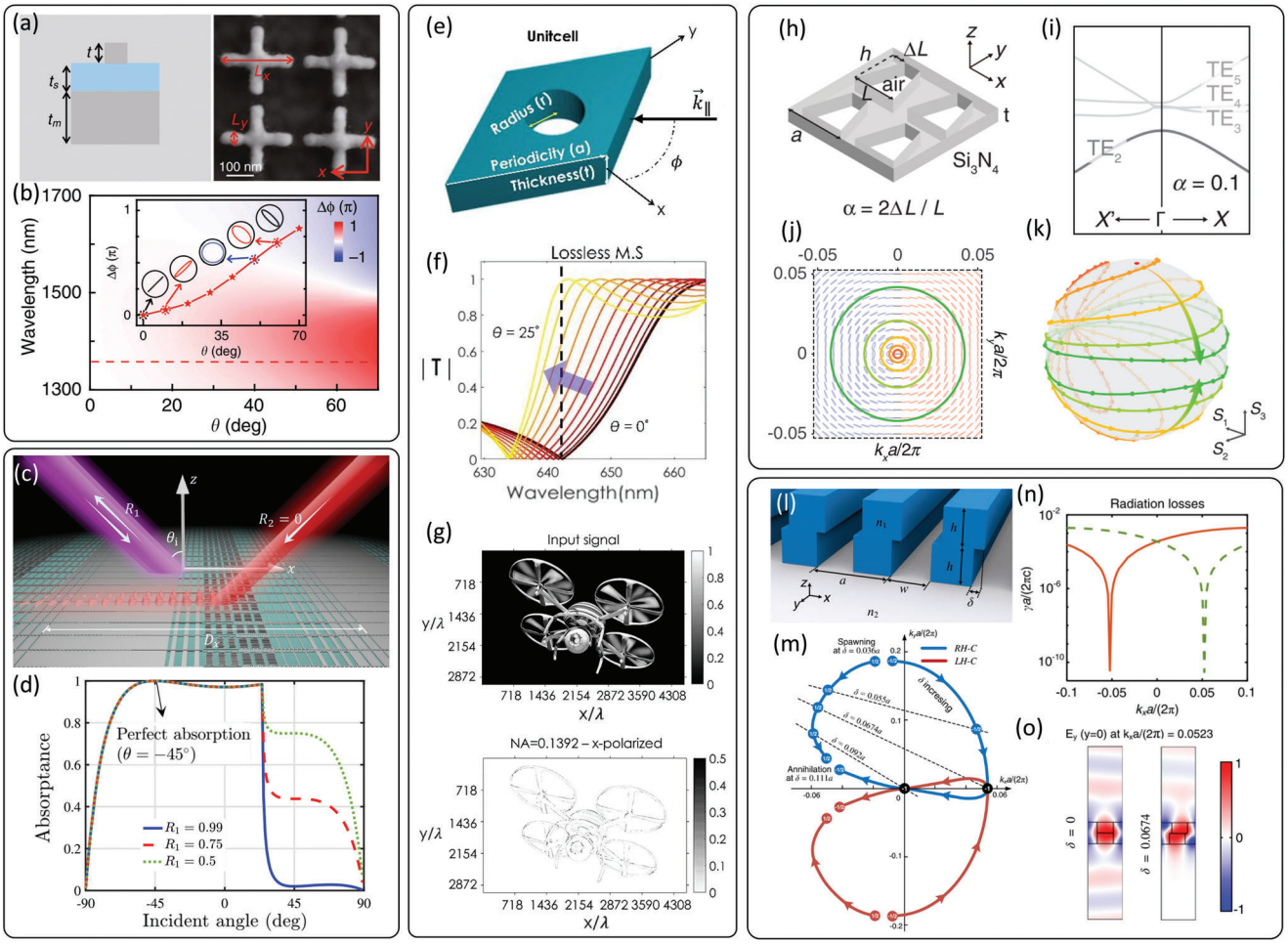

Figure 5. Optical manipulation in the momentum domain. a,b) An angle-multiplexed meta-polarizer based on angular dispersion manipulation. a) Side view schematic (left plane) and top-view SEM image (right plane) of the designed metasurface. b) Simulated phase difference between TE and TM reflection waves as a function of wavelength and incident angle. Inset: The phase difference between TE and TM reflection waves as a function of incident angle at the wavelength of 1358 nm, demonstrating that the polarization state of reflected waves can be manipulated by changing the incident angle. c,d) Angular-asymmetric absorption based on gradient metasurfaces. c) Schematic of the gradient metasurface as the asymmetric absorber. d) Numerically calculated absorptance as a function of the incident angle for different reflection coefficients. e–g) Polarization-insensitive metasurfaces for second-order analog mathematical operation on optical images. e) Schematic of a unit cell of the polarization-insensitive metasurface. f) Transmission spectra of the lossless polarization-insensitive metasurface for *y*-polarized waves propagation in the *x*–*z* plane (θ represents the angle between the wave propagation direction and the *z*-axis). g) The 2D image (upper planer) and the output (bottom plane) after the metasurface for *x*-polarized waves. h–k) Circular polarization states spawning from bound states in the continuum. h) Schematic of the structure and the definition of asymmetry parameter α. i) The TE-like band structure of the designed structure with $\alpha = 0.1$. The circular loops of polarization states mapped from j) the Brillouin zone to k) the Poincare sphere. l–o) Manipulating the topological polarization singularity in the momentum space. l) Schematic of the 1D photonic crystal slab and the definition of the misalignment δ. m) Variation of the polarization singularities with the changing of δ for downward radiation. n) Radiation losses from eigenmodes as a function of k_x toward the top (orange) and bottom (dashed green) of the structure with $\delta = 0.0674a$. o) Electric field profiles (*y*-component) of the eigenmodes. Panels reproduced with permission from: a,b) Reproduced with permission.[164] Copyright 2020, Springer Nature. c,d) Reproduced with permission.[166] Copyright 2018, American Physical Society. e–g) Reproduced with permission.[170] Copyright 2020, American Chemical Society. h–k) Reproduced with permission.[23] Copyright 2019, American Physical Society. l–o) Reproduced with permission.[175] Copyright 2021, American Physical Society.

6.3. Optical Manipulation in the Momentum Space Based on BICs

Later, the topological nature of BICs emerged as a powerful alternative for optical manipulation in the momentum space.[19,20,172] The BICs represent the singular points of polarizations in the momentum space, which refers to the centers of polarization vortices (*V* points). Metasurfaces with *V* points have been used to generate optical vortex beams.[173] Compared with traditional devices for optical vortex generation, such as spiral phase plates and phased antenna arrays, metasurfaces with *V* points are homogeneous without real-space centers. This key feature is quite beneficial to real applications because there is no need to align the center of optical device with the optical beam center. Furthermore, by continuously varying the structure parameters of photonic nanostructures, the *V* points can split into two *C* points

(corresponding to the circular-polarized eigenmodes) complying with the law of topological charge conservation. As a result, the polarization states of far-field radiations can be manipulated with a high degree of freedom. For example, a 2D photonic crystal slab without C_{2z} rotation symmetry (as shown in Figure 5h) was proposed to manipulate the polarization states of far-field radiations with different k vectors.[23] By changing the asymmetric structural parameter α, the in-plane inversion C_2 symmetry of the photonic crystal slab is broken, resulting in the split of the at-Γ V point of band TE_2 (as shown in Figure 5i) into two C points with opposite chirality. The two C points are very close to the Γ point, clamping an L line, as shown in Figure 5j. For circular loops with different radii, the polarization state continuously changes along the loops, and full Poincare sphere coverage can be realized, as shown in Figure 5k. Therefore, the polarization state of far-field radiation can be well manipulated by controlling the V and C points in the momentum space. Besides the polarization state of far-field radiation, the direction of far-field radiation can also be manipulated based on photonic nanostructures without σ_z symmetry by controlling the singular points of polarizations in the momentum space.[174,175] Figure 5l shows a 1D photonic crystal slab with asymmetric structural parameter δ describing the misalignment between the two superimposed identical gratings along the x-direction. By continuously varying δ, the singular points of polarizations can be manipulated in the momentum space, as shown in Figure 5m,n. At some fixed values of δ, the forward or the backward radiation loss is close to zero for fixed k vectors, resulting in unidirectional far-field radiation. These works demonstrate that the properties of far-field radiations can be well controlled based on the manipulation of singular points of polarizations in the momentum space.

7. Outlook and Conclusions

Multidimensional manipulation of optical waves based on metasurfaces has witnessed the rapid development of optical and photonic manipulation in the past decade, which promotes the miniaturization and integration of optical devices and has shown great application potential for light generation, manipulation, and detection. Recently, metasurfaces have been applied in the design of integrated photonic light sources. Low-threshold laser emission, vortex laser arrays, chiral light emission, and quantum sources have been realized based on metasurfaces.[9,176–178] Benefit from their excellent ability in optical field manipulation, metasurfaces have been widely used for the realization of novel integrated photonic devices, such as dispersion-controlled metalenses, multi-color hologram, computational photonic elements, integrated quantum photonic systems, and so on.[90,168,179,180] Metasurfaces have also shown great advantages for the detection of optical fields and ultra-sensitive optical biosensing.[181,182] Precise measurement of amplitude, phase, polarization state, wavefront, and OAM of optical waves has been well demonstrated in metasurface-based optical devices and systems.[183–187] Predictably, metasurface-integrated photonic devices and systems with novel optical functionalities and various integrated optical functionalities will further expand the application of metasurfaces and promote the development of optics and photonics.

aDespite the great progress made in the study of optical multidimensional optical field manipulation based on metasurfaces in the last two decades, there are still some open challenges that need to be addressed to further expand the functionality of metasurfaces and promote their commercial application. Efficient approaches to realize the integration and application of metasurfaces in on-chip and hybrid photonic systems are still highly desirable, which play a key role in the real application of metasurfaces.[188,189] Exploring the capacity of metasurfaces in the implementation of novel optical functionalities will further promote the development of meta-optics.[190] Recent development in active metasurfaces demonstrated that metasurfaces are not only good candidates for the realization of integration and miniaturization of photonic devices, but also powerful platforms to implement intelligent photonic devices.[191–193] Dynamic metasurfaces in which the optical responses of every nanostructure can be independently modulated have rarely been presented in the visible and near-infrared regimes. Meanwhile, for metasurfaces' design and optimization, recent approaches always establish meta-atom libraries by varying the structural parameters of several nanostructures in certain ranges, and find the appropriate nanostructures from the libraries to constitute the metasurfaces with desired optical functionalities.[69,194] The coverage of the meta-atom libraries becomes a major constraint on the efficient design of metasurfaces. To realize optical multidimensional manipulation, both the linear and nonlinear optical responses of nanostructures in real space, momentum space, and other dimensions need to be considered. Expanding the design freedom of nanostructures (such as introducing multiple constitute materials, using multi-layer design, and so on) in meta-atom libraries is essential. Otherwise, realizing the inverse design of nanostructures based on the desired optical responses is another way to solve this challenge. For the design of large-area aperiodic metasurfaces with non-negligible interactions between nanostructures, quantitative description and global optimization of non-local interactions between different nanostructures is essential, which may significantly affect the actual performance of metasurfaces. The fabrication technologies of metasurfaces need to be further improved to realize metasurfaces with a large area, fine structures, and accurately aligned multiple layers.

Here we envision several future directions that the multidimensional optical field manipulation may have a profound impact.

7.1. 3D Structured Light with Evolution along the Optical Path

Recently, 3D structured light has drawn much attention from researchers because such special light fields can carry bulky optical information such as the toroidal vortices of light and controllable transverse OAM generation.[195,196] One main challenge to artificially modulate the optical fields along the optical path is the lack of design principle because the propagation term in the wave functions is usually isolated especially under the paraxial approximation. Dorrah et al. demonstrated on-demand polarization transformation along the optical path using multiple Bessel beams generation.[197] Different from conventional polarization-based optical effects, which maintain their polarization states during light propagation, this effect enables polarization evolution along the optical path in an artificially designed manner. Thus, the optical propagation direction serves as a new degree

of freedom for optical manipulation. Furthermore, when considering the vortex wave-front of the generated multi-Bessel beams, the OAM of light can also be structured along the propagation direction with spatially controlled polarization states.[198,199] The optical structures with evolution along the optical path may lead to informational designs such as information encryption in different locations and 3D holographic plates.

7.2. Ultra-Fast Control of the Optical Fields in Multidimensions

One of the most fundamental challenges of optical metasurfaces is how to realize ultra-fast control of their functions. In the past few years, researchers have endeavored to find different schemes to realize reconfigurable metasurfaces, such as using phase–changing materials,[200] infiltrating liquid crystal around nanostructures,[201] adopting micro-electromechanical systems,[202] and using EM gating of the building blocks,[203] which enable manipulating different optical properties at different time. Basically, reconfigurable metasurfaces require either tuning the properties of the building blocks such as their constitution materials and shapes, or modulating the operating environment of the optical elements such as varying the incident light and the substrate. To date, ultra-fast control of optical waves in combined optical dimensions remains a challenge. One of the strategies to achieve ultra-fast control of optical fields is using optical-induced methods, such as frequency-gradient metasurfaces that can vary the steering angle of 25° in just 8 picoseconds.[204] With the rapid development of material science and fabrication technology, thin-film-based lithium niobate has been severing as a potential candidate for ultra-fast optical manipulation. For example, Lin et al. realized fast polarization scrambling on the Poincaré sphere with a speed reaching 65 Mrad s^{-1} and a polarization extinction ratio up to 41.9 dB based on thin-film lithium niobate.[205]

7.3. Optical Multidimensional Manipulation Based on Global Optimized Metasurfaces

In traditional approaches, the design and optimization of metasurfaces are always based on an interactive process of trial and error using numerical simulations, which is time–consuming and require a significant amount of professional knowledge when the design goal is complex. Therefore, current optimization methods by solving Maxwell's functions are not good candidates for the design and optimization of metasurfaces for the realization of multidimensional manipulation of optical waves since the design goal is very complex. Very recently, artificial intelligence has been utilized in nanophotonics to realize the design of metasurfaces. Lately, approaches have well demonstrated that metasurface optimization methods based on artificial intelligence provide powerful platforms for the prediction of the optical responses of metasurfaces and the inverse design of metasurfaces.[206–208] Compared with traditional methods, they have comparable accuracy, reduce the requirement on professional knowledge and significantly increase computation efficiency. By utilizing both gradient-based and gradient-free optimization techniques, inverse design methods based on deep learning have been widely applied for the inverse design of both periodic and aperiodic metasurfaces.[159,209] Importantly, artificial intelligence shows unprecedented possibilities for the optimization and inverse design of large-area aperiodic metasurfaces composed of nanostructures with non-negligible local and nonlocal interactions.[210–212] The rapid development in artificial intelligence has boosted the discovery of novel photonic effects, device design, and information post-processing.[213] Empowered by the topological optimization method and other artificial intelligence technology, one can realize peculiar photonic devices such as high-efficiency and large-NA metalens,[63] inversely designed functional metasurfaces,[214] reprogrammable metasurface imagers,[215] programmable diffractive deep neural network based on metasurfaces,[216] deep learning based single-shot autofocus microscopy,[217] and bidirectional deep neural network for structural colors generation.[143] Overall, the current inverse design methods work through finding the relationship between the structural parameters of nanostructures and their limited optical responses. To further realize the inverse design of metasurfaces for multidimensional manipulation of optical waves, the capabilities of current inverse design methods need to be further expanded by adding more degrees of freedom. With the future combination of optical manipulation, device fabrication, and optical detection through a globally optimized artificial intelligence technique, one can envision a broad area for efficient and multifunctional metasurfaces with lower power consumption and high integration.

8. Conclusions

In this review article, we have presented an overview of metasurface-based optical field manipulation in multidimensions. We started by reviewing the basic phenomenological properties of optical sub-wavelength resonators and summarized the local resonances and modes coupling generated by the nanostructures for optical field manipulation. We have shown that metasurfaces with elaborate designs can realize abundant local resonances that lead to tremendous applications such as metalens and holography. When the optical resonances are induced by the symmetry or other global effects of the nanostructure arrays, nonlocal resonances can be generated to support high Q factor applications and achieve efficient wave-front control with specific dispersions. Modes coupling also occurs between the nonlocal modes and local modes, which offers rich opportunities to engineer the overall scattering properties of nanostructures. We discussed the definition of optical manipulation in multidimensions and expanded the optical dimensions to more generalized ones that can carry different information channels. We then continued our discussion to more specific categories such as phase-based, polarization-based, wavelength-based, and momentum-based optical manipulation. We summarized the phase-based multi-wave-front manipulation for wave-front compensation, orthogonal-basis-based OAM channels for information transmission, disorder engineer wave-front control for spatial coherence modulation, and nonlinear wave-front manipulation. By considering the combination of different polarization channels, we discussed orthogonal polarization multiplexing, discrete, continuous, and customized multidimensional manipulation. We also extended our discussion to other

multidimensions such as wavelength-selective and momentum-selective multi-functional optical manipulation and the corresponding applications. Finally, we envisioned several research directions that may have a profound impact in the upcoming future. A detailed discussion of these research fields goes beyond the scope of this paper, but the discussion highlights the rich effects and phenomena that may benefit the whole research area of the metasurfaces. The development in this realm will continuously reveal more and more compelling and fascinating optical designs and bring in new opportunities in photonics and interdisciplinary research.

Acknowledgements

W.L., Z.L., and M.A.A. contributed equally to this work. This work was supported by the National Key Research and Development Program of China (2021YFA1400601 and 2022YFA1404501), the National Natural Science Fund for Distinguished Young Scholar (11925403), the National Natural Science Foundation of China (12122406, 12192253, 11974193, 12274237, 12274239, and U22A20258), and the 111 Project of B23045. X.C. would like to acknowledge the support from the Leverhulme Trust (RPG-2021-145), RSE International Exchange Programme: RSE—NSFC Joint Projects, and the Royal Society International Exchanges (IES\R3\193046).

Conflict of Interest

The authors declare no conflict of interest.

Keywords

metasurfaces, multidimensions, multi-functions, optical field manipulation

Received: September 27, 2022
Revised: March 7, 2023
Published online:

[1] N. Yu, P. Genevet, M. A. Kats, F. Aieta, J. P. Tetienne, F. Capasso, Z. Gaburro, *Science* **2011**, *334*, 333.
[2] T. Xu, A. Agrawal, M. Abashin, K. J. Chau, H. J. Lezec, *Nature* **2013**, *497*, 470.
[3] X. Yin, Z. Ye, J. Rho, Y. Wang, X. Zhang, *Science* **2013**, *339*, 1405.
[4] N. Landy, D. R. Smith, *Nat. Mater.* **2013**, *12*, 25.
[5] J. Mun, M. Kim, Y. Yang, T. Badloe, J. Ni, Y. Chen, C.-W. Qiu, J. Rho, *Light: Sci. Appl.* **2020**, *9*, 139.
[6] S. P. Rodrigues, S. Lan, L. Kang, Y. Cui, P. W. Panuski, S. Wang, A. M. Urbas, W. Cai, *Nat. Commun.* **2017**, *8*, 14602.
[7] X. Chen, L. Huang, H. Muhlenbernd, G. Li, B. Bai, Q. Tan, G. Jin, C. W. Qiu, S. Zhang, T. Zentgraf, *Nat. Commun.* **2012**, *3*, 1198.
[8] M. Khorasaninejad, W. T. Chen, R. C. Devlin, J. Oh, A. Y. Zhu, F. Capasso, *Science* **2016**, *352*, 1190.
[9] W. Liu, Z. Li, H. Cheng, C. Tang, J. Li, S. Zhang, S. Chen, J. Tian, *Adv. Mater.* **2018**, *30*, 1706368.
[10] A. Y. Zhu, W. T. Chen, A. Zaidi, Y. W. Huang, M. Khorasaninejad, V. Sanjeev, C.-W. Qiu, F. Capasso, *Light: Sci. Appl.* **2018**, *7*, 17158.
[11] E. W. Wang, T. Phan, S. J. Yu, S. Dhuey, J. A. Fan, *Proc. Natl. Acad. Sci. U. S. A.* **2022**, *119*, e2122085119.
[12] X. Zang, F. Dong, F. Yue, C. Zhang, L. Xu, Z. Song, M. Chen, P.-Y. Chen, G. S. Buller, Y. Zhu, S. Zhuang, W. Chu, S. Zhang, X. Chen, *Adv. Mater.* **2018**, *30*, 1707499.
[13] Y. Bao, Y. Yu, H. Xu, C. Guo, J. Li, S. Sun, Z. K. Zhou, C.-W. Qiu, X. H. Wang, *Light: Sci. Appl.* **2019**, *8*, 95.
[14] I. Kim, J. Jang, G. Kim, J. Lee, T. Badloe, J. Mun, J. Rho, *Nat. Commun.* **2021**, *12*, 3614.
[15] Q. Fan, W. Zhu, Y. Liang, P. Huo, C. Zhang, A. Agrawal, K. Huang, X. Luo, Y. Lu, C.-W. Qiu, H. J. Lezec, T. Xu, *Nano Lett.* **2019**, *19*, 1158.
[16] M. V. Rybin, K. L. Koshelev, Z. F. Sadrieva, K. B. Samusev, A. A. Bogdanov, M. F. Limonov, Y. S. Kivshar, *Phys. Rev. Lett.* **2017**, *119*, 243901.
[17] S. Liu, A. Vaskin, S. Campione, O. Wolf, M. B. Sinclair, J. Reno, G. A. Keeler, I. Staude, I. Brener, *Nano Lett.* **2017**, *17*, 4297.
[18] K. Koshelev, Y. Kivshar, *ACS Photonics* **2020**, *8*, 102.
[19] B. Zhen, C. W. Hsu, L. Lu, A. D. Stone, M. Soljačić, *Phys. Rev. Lett.* **2014**, *113*, 257401.
[20] K. Koshelev, S. Lepeshov, M. Liu, A. Bogdanov, Y. Kivshar, *Phys. Rev. Lett.* **2018**, *121*, 193903.
[21] C. W. Hsu, B. Zhen, A. D. Stone, J. D. Joannopoulos, M. Soljačić, *Nat. Rev. Mater.* **2016**, *1*, 16048.
[22] Z. Che, Y. Zhang, W. Liu, M. Zhao, J. Wang, W. Zhang, F. Guan, X. Liu, W. Liu, L. Shi, J. Zi, *Phys. Rev. Lett.* **2021**, *127*, 043901.
[23] W. Liu, B. Wang, Y. Zhang, J. Wang, M. Zhao, F. Guan, X. Liu, L. Shi, J. Zi, *Phys. Rev. Lett.* **2019**, *123*, 116104.
[24] J. Jin, X. Yin, L. Ni, M. Soljačić, B. Zhen, C. Peng, *Nature* **2019**, *574*, 501.
[25] M. Kang, S. Zhang, M. Xiao, H. Xu, *Phys. Rev. Lett.* **2021**, *126*, 117402.
[26] T. Yoda, M. Notomi, *Phys. Rev. Lett.* **2020**, *125*, 053902.
[27] M. V. Gorkunov, A. A. Antonov, Y. S. Kivshar, *Phys. Rev. Lett.* **2020**, *125*, 093903.
[28] M. V. Gorkunov, A. A. Antonov, V. R. Tuz, A. S. Kupriianov, Y. S. Kivshar, *Adv. Opt. Mater.* **2021**, *9*, 2100797.
[29] Q. Song, J. Hu, S. Dai, C. Zheng, D. Han, J. Zi, Z. Q. Zhang, C. T. Chan, *Sci. Adv.* **2020**, *6*, eabc1160.
[30] K. Koshelev, S. Kruk, E. Melik-Gaykazyan, J. H. Choi, A. Bogdanov, H. G. Park, Y. Kivshar, *Science* **2020**, *367*, 288.
[31] C. Fang, Q. Yang, Q. Yuan, L. Gu, X. Gan, Y. Shao, Y. Liu, G. Han, Y. Hao, *Laser Photonics Rev.* **2022**, *16*, 2100498.
[32] X. Chen, L. Huang, H. Mühlenbernd, G. Li, B. Bai, Q. Tan, G. Jin, C.-W. Qiu, S. Zhang, T. Zentgraf, *Nat. Commun.* **2012**, *3*, 1198.
[33] S. Chen, Z. Li, W. Liu, H. Cheng, J. Tian, *Adv. Mater.* **2019**, *31*, 1802458.
[34] V. Ginis, M. Piccardo, M. Tamagnone, J. Lu, M. Qiu, S. Kheifets, F. Capasso, *Science* **2020**, *369*, 436.
[35] X. Ding, F. Monticone, K. Zhang, L. Zhang, D. Gao, S. N. Burokur, A. Lustra, Q. Wu, C.-W. Qiu, A. Alù, *Adv. Mater.* **2015**, *27*, 1195.
[36] M. Khorasaninejad, F. Capasso, *Science* **2017**, *358*, eaam8100.
[37] A. Arbabi, Y. Horie, M. Bagheri, A. Faraon, *Nat. Nanotechnol.* **2015**, *10*, 937.
[38] J. B. Mueller, N. A. Rubin, R. C. Devlin, B. Groever, F. Capasso, *Phys. Rev. Lett.* **2017**, *118*, 113901.
[39] W. Ye, F. Zeuner, X. Li, B. Reineke, S. He, C.-W. Qiu, J. Liu, Y. Wang, S. Zhang, T. Zentgraf, *Nat. Commun.* **2016**, *7*, 11930.
[40] M. Ma, Z. Li, W. Liu, C. Tang, Z. Li, H. Cheng, J. Li, S. Chen, J. Tian, *Laser Photonics Rev.* **2019**, *13*, 1900045.
[41] F. Yue, D. Wen, C. Zhang, B. D. Gerardot, W. Wang, S. Zhang, X. Chen, *Adv. Mater.* **2017**, *29*, 1603838.
[42] W. Liu, Z. Li, Z. Li, H. Cheng, C. Tang, J. Li, S. Chen, J. Tian, *Adv. Mater.* **2019**, *31*, 1901729.
[43] Z. Hao, W. Liu, Z. Li, Z. Li, G. Geng, Y. Wang, H. Cheng, H. Ahmed, X. Chen, J. Li, J. Tian, S. Chen, *Laser Photonics Rev.* **2021**, *15*, 2100207.
[44] H. L. Wang, H. F. Ma, M. Chen, S. Sun, T. J. Cui, *Adv. Funct. Mater.* **2021**, *31*, 2100275.
[45] Z. Li, W. Liu, H. Cheng, D. Y. Choi, S. Chen, J. Tian, *Adv. Mater.* **2020**, *32*, 1907983.

[46] M. Liu, E. Plum, H. Li, S. Duan, S. Li, Q. Xu, X. Zhang, C. Zhang, C. Zou, B. Jin, J. Han, W. Zhang, *Adv. Opt. Mater.* **2020**, *8*, 2000247.
[47] Y. Ding, X. Chen, Y. Duan, H. Huang, L. Zhang, S. Chang, X. Guo, X. Ni, *ACS Photonics* **2022**, *9*, 398.
[48] L. Huang, X. Chen, H. Mühlenbernd, G. Li, B. Bai, Q. Tan, G. Jin, T. Zentgraf, S. Zhang, *Nano Lett.* **2012**, *12*, 5750.
[49] J. Zhou, T. Koschny, M. Kafesaki, E. N. Economou, J. B. Pendry, C. M. Soukoulis, *Phys. Rev. Lett.* **2005**, *95*, 223902.
[50] Y. Kivshar, *Nano Lett.* **2022**, *22*, 3513.
[51] Y. Chen, X. Yang, J. Gao, *Light: Sci. Appl.* **2018**, *7*, 84.
[52] B. Yang, W. Liu, Z. Li, H. Cheng, D. Y. Choi, S. Chen, J. Tian, *Nano Lett.* **2019**, *19*, 4221.
[53] M. F. Limonov, M. V. Rybin, A. N. Poddubny, Y. S. Kivshar, *Nat. Photonics* **2017**, *11*, 543.
[54] A. A. Bogdanov, K. L. Koshelev, P. V. Kapitanova, M. V. Rybin, S. A. Gladyshev, Z. F. Sadrieva, K. B. Samusev, Y. S. Kivshar, M. F. Limonov, *Adv. Photonics* **2019**, *1*, 016001.
[55] K. Koshelev, A. Bogdanov, Y. Kivshar, *Opt. Photonics News* **2020**, *31*, 38.
[56] Z. L. Deng, F. J. Li, H. Li, X. Li, A. Alù, *Laser Photonics Rev.* **2022**, *16*, 2100617.
[57] G. Yang, S. U. Dev, M. S. Allen, J. W. Allen, H. Harutyunyan, *Nano Lett.* **2022**, *22*, 2001.
[58] Z. Liu, Y. Xu, Y. Lin, J. Xiang, T. Feng, Q. Cao, J. Li, S. Lan, J. Liu, *Phys. Rev. Lett.* **2019**, *123*, 253901.
[59] R. Chai, W. Liu, Z. Li, H. Cheng, J. Tian, S. Chen, *Phys. Rev. B* **2021**, *104*, 075149.
[60] M. Lawrence, D. R. Barton III, J. Dixon, J. H. Song, J. van de Groep, M. L. Brongersma, J. A. Dionne, *Nat. Nanotechnol.* **2020**, *15*, 956.
[61] E. Klopfer, M. Lawrence, D. R. Barton III, J. Dixon, J. A. Dionne, *Nano Lett.* **2020**, *20*, 5127.
[62] A. C. Overvig, S. C. Malek, N. Yu, *Phys. Rev. Lett.* **2020**, *125*, 017402.
[63] T. Phan, D. Sell, E. W. Wang, S. Doshay, K. Edee, J. Yang, J. A. Fan, *Light: Sci. Appl.* **2019**, *8*, 48.
[64] E. Maguid, I. Yulevich, D. Veksler, V. Kleiner, M. L. Brongersma, E. Hasman, *Science* **2016**, *352*, 1202.
[65] Q. Fan, M. Liu, C. Zhang, W. Zhu, Y. Wang, P. Lin, F. Yan, L. Chen, H. J. Lezec, Y. Lu, A. Agrawal, T. Xu, *Phys. Rev. Lett.* **2020**, *125*, 267402.
[66] Y. Bao, L. Wen, Q. Chen, C.-W. Qiu, B. Li, *Sci. Adv.* **2021**, *7*, eabh0365.
[67] H. X. Xu, G. Hu, L. Han, M. Jiang, Y. Huang, Y. Li, X. Yang, X. Ling, L. Chen, J. Zhao, C.-W. Qiu, *Adv. Opt. Mater.* **2018**, *6*, 1801479.
[68] M. Kim, A. M. Wong, G. V. Eleftheriades, *Phys. Rev. X* **2014**, *4*, 041042.
[69] A. C. Overvig, S. Shrestha, S. C. Malek, M. Lu, A. Stein, C. Zheng, N. Yu, *Light: Sci. Appl.* **2019**, *8*, 92.
[70] L. Liu, W. Liu, F. Wang, H. Cheng, D. Y. Choi, J. Tian, Y. Cai, S. Chen, *Nano Lett.* **2022**, *22*, 6342.
[71] S. M. Kamali, E. Arbabi, A. Arbabi, Y. Horie, M. Faraji-Dana, A. Faraon, *Phys. Rev. X* **2017**, *7*, 041056.
[72] X. Ouyang, Y. Xu, M. Xian, Z. Feng, L. Zhu, Y. Cao, S. Lan, B.-O. Guan, C.-W. Qiu, X. Li, *Nat. Photonics* **2021**, *15*, 901.
[73] S. Wang, P. C. Wu, V. C. Su, Y. C. Lai, C. H. Chu, J. W. Chen, S. H. Lu, J. Chen, B. Xu, C.-H. Kuan, T. Li, S. Zhu, D. P. Tsai, *Nat. Commun.* **2017**, *8*, 187.
[74] C. Min, J. Liu, T. Lei, G. Si, Z. Xie, J. Lin, L. Du, X. Yuan, *Laser Photonics Rev.* **2016**, *10*, 978.
[75] A. Arbabi, E. Arbabi, S. M. Kamali, Y. Horie, S. Han, A. Faraon, *Nat. Commun.* **2016**, *7*, 13682.
[76] B. Groever, W. T. Chen, F. Capasso, *Nano Lett.* **2017**, *17*, 4902.
[77] W. Liu, D. Ma, Z. Li, H. Cheng, D. Y. Choi, J. Tian, S. Chen, *Optica* **2020**, *7*, 1706.
[78] W. T. Chen, A. Y. Zhu, V. Sanjeev, M. Khorasaninejad, Z. Shi, E. Lee, F. Capasso, *Nat. Nanotechnol.* **2018**, *13*, 220.
[79] Y. Wang, Q. Chen, W. Yang, Z. Ji, L. Jin, X. Ma, Q. Song, A. Boltasseva, J. Han, V. M. Shalaev, S. Xiao, *Nat. Commun.* **2021**, *12*, 5560.
[80] R. C. Devlin, A. Ambrosio, N. A. Rubin, J. B. Mueller, F. Capasso, *Science* **2017**, *358*, 896.
[81] Q. Song, M. Odeh, J. Zúñiga-Pérez, B. Kanté, P. Genevet, *Science* **2021**, *373*, 1133.
[82] H. Ren, G. Briere, X. Fang, P. Ni, R. Sawant, S. Héron, S. Chenot, S. Vézian, B. Damilano, V. Brändli, S. A. Maier, P. Genevet, *Nat. Commun.* **2019**, *10*, 2986.
[83] H. Ren, X. Fang, J. Jang, J. Bürger, J. Rho, S. A. Maier, *Nat. Nanotechnol.* **2020**, *15*, 948.
[84] Z. H. Jiang, L. Kang, W. Hong, D. H. Werner, *Phys. Rev. Appl.* **2018**, *9*, 064009.
[85] Y. Eliezer, G. Qu, W. Yang, Y. Wang, H. Yılmaz, S. Xiao, Q. Song, H. Cao, *Light: Sci. Appl.* **2021**, *10*, 104.
[86] S. Chen, G. Li, F. Zeuner, W. H. Wong, E. Y. B. Pun, T. Zentgraf, S. Zhang, *Phys. Rev. Lett.* **2014**, *113*, 033901.
[87] G. Li, S. Chen, N. Pholchai, B. Reineke, P. W. H. Wong, E. Y. B. Pun, K. W. Cheah, T. Zentgraf, S. Zhang, *Nat. Mater.* **2015**, *14*, 607.
[88] C. Schlickriede, S. S. Kruk, L. Wang, B. Sain, Y. Kivshar, T. Zentgraf, *Nano Lett.* **2020**, *20*, 4370.
[89] T. Todorov, L. Nikolova, K. Stoyanova, N. Tomova, *Appl. Opt.* **1985**, *24*, 785.
[90] Z. L. Deng, Z. Q. Wang, F. J. Li, M. X. Hu, X. Li, *Nanophotonics* **2022**, *11*, 1725.
[91] Q. Song, X. Liu, C.-W. Qiu, P. Genevet, *Appl. Phys. Rev.* **2022**, *9*, 011311.
[92] R. Zhao, L. Huang, Y. Wang, *PhotoniX* **2020**, *1*, 20.
[93] M. A. Naveed, J. Kim, I. Javed, M. A. Ansari, J. Seong, Y. Massoud, T. Badloe, I. Kim, K. Riaz, M. Zubair, M. Q. Mehmood, J. Rho, *Adv. Opt. Mater.* **2022**, *10*, 2200196.
[94] H. S. Khaliq, M. R. Akram, K. Riaz, M. A. Ansari, J. Akbar, J. Zhang, W. Zhu, D. Zhang, X. Wang, M. Zubair, M. Q. Mehommd, *Opt. Express* **2021**, *29*, 3230.
[95] A. S. Rana, I. Kim, M. A. Ansari, M. S. Anwar, M. Saleem, T. Tauqeer, A. Danner, M. Zubair, M. Q. Mehmood, J. Rho, *ACS Appl. Mater. Interfaces* **2020**, *12*, 48899.
[96] M. A. Ansari, I. Kim, D. Lee, M. H. Waseem, M. Zubair, N. Mahmood, T. Badloe, S. Yerci, T. Tauqeer, M. Q. Mehmood, J. Rho, *Laser Photonics Rev.* **2020**, *13*, 1900065.
[97] M. A. Ansari, T. Tauqeer, M. Zubair, M. Q. Mehmood, *Nanophotonics* **2020**, *9*, 963.
[98] L. Nikolova, P. S. Ramanujam, *Polarization Holography*, Cambridge University Press, Cambridge **2009**.
[99] D. Wen, F. Yue, G. Li, G. Zheng, K. Chan, S. Chen, M. Chen, K. F. Li, P. W. H. Wong, K. W. Cheah, E. Y. B. Pun, S. Zhang, X. Chen, *Nat. Commun.* **2015**, *6*, 8241.
[100] I. Kim, M. A. Ansari, M. Q. Mehmood, W. S. Kim, J. Jang, M. Zubair, Y.-K. Kim, J. Rho, *Adv. Mater.* **2020**, *32*, 2004664.
[101] I. Kim, W. S. Kim, K. Kim, M. A. Ansari, M. Q. Mehmood, T. Badloe, Y. Kim, J. Gwak, H. Lee, Y.-K. Kim, J. Rho, *Sci. Adv.* **2021**, *7*, eabe9943.
[102] M. A. Ansari, I. Kim, I. D. Rukhlenko, M. Zubair, S. Yerci, T. Tauqeer, M. Q. Mehmood, J. Rho, *Nanoscale Horiz.* **2020**, *5*, 57.
[103] M. A. Naveed, M. A. Ansari, I. Kim, T. Badloe, J. Kim, D. K. Oh, K. Riaz, T. Tauqeer, U. Younis, M. Saleem, M. S. Anwar, M. Zubair, M. Q. Mehmood, J. Rho, *Microsyst. Nanoeng.* **2021**, *7*, 5.
[104] M. A. Ansari, M. A. Naveed, M. Zubair, M. Q. Mehmood, in *1st Int. Conf. on Microwave, Antennas & Circuits (ICMAC)*, IEEE, Piscataway, NJ **2021**, pp. 1–3.
[105] F. Zhang, M. Pu, X. Li, P. Gao, X. Ma, J. Luo, H. Yu, X. Luo, *Adv. Funct. Mater.* **2017**, *27*, 1704295.
[106] Z. Shi, N. A. Rubin, J. S. Park, F. Capasso, *Phys. Rev. Lett.* **2022**, *129*, 167403.

[107] J. Deng, L. Deng, Z. Guan, J. Tao, G. Li, Z. Li, Z. Li, S. Yu, G. Zheng, *Nano Lett.* **2020**, *20*, 1830.
[108] Z. L. Deng, J. Deng, X. Zhuang, S. Wang, K. Li, Y. Wang, Y. Chi, X. Ye, J. Xu, G. P. Wang, R. Zhao, X. Wang, Y. Cao, X. Cheng, G. Li, X. Li, *Nano Lett.* **2018**, *18*, 2885.
[109] D. Wen, J. J. Cadusch, J. Meng, K. B. Crozier, *Nano Lett.* **2021**, *21*, 1735.
[110] N. A. Rubin, A. Zaidi, A. H. Dorrah, Z. Shi, F. Capasso, *Sci. Adv.* **2021**, *7*, eabg7488.
[111] Q. Song, A. Baroni, P. C. Wu, S. Chenot, V. Brandli, S. Vézian, B. Damilano, P. de Mierry, S. Khadir, P. Ferrand, P. Genevet, *Nat. Commun.* **2021**, *12*, 3631.
[112] E. Arbabi, S. M. Kamali, A. Arbabi, A. Faraon, *ACS Photonics* **2019**, *6*, 2712.
[113] X. Guo, J. Zhong, B. Li, S. Qi, Y. Li, P. Li, D. Wen, S. Liu, B. Wei, J. Zhao, *Adv. Mater.* **2022**, *34*, 2103192.
[114] Z. L. Deng, M. Jin, X. Ye, S. Wang, T. Shi, J. Deng, N. Mao, Y. Cao, B-O. Guan, A. Alù, G. Li, X. Li, *Adv. Funct. Mater.* **2020**, *30*, 1910610.
[115] N. Zhao, Z. Li, G. Zhu, J. Li, L. Deng, Q. Dai, W. Zhang, Z. He, G. Zheng, *Opt. Express* **2022**, *30*, 37554.
[116] R. Wang, Y. Intaravanne, S. Li, J. Han, S. Chen, J. Liu, S. Zhang, L Li, X. Chen, *Nano Lett.* **2021**, *21*, 2081.
[117] X. Zang, H. Ding, Y. Intaravanne, L. Chen, Y. Peng, J. Xie, Q. Ke, A. V. Balakin, A. P. Shkurinov, X. Chen, Y. Zhu, S. Zhuang, *Laser Photonics Rev.* **2019**, *13*, 1900182.
[118] R. Wang, G. Ren, Z. Ren, J. Liu, S. Li, X. Chen, L. Li, *Opt. Express* **2022**, *30*, 7137.
[119] A. Kristensen, J. K. Yang, S. I. Bozhevolnyi, S. Link, P. Nordlander, N. J. Halas, N. A. Mortensen, *Nat. Rev. Mater.* **2017**, *2*, 16088.
[120] D. Franklin, S. Modak, A. Vázquez-Guardado, A. Safaei, D. Chanda, *Light: Sci. Appl.* **2018**, *7*, 93.
[121] J. Xue, Z. K. Zhou, L. Lin, C. Guo, S. Sun, D. Lei, C.-W. Qiu, X. H. Wang, *Light: Sci. Appl.* **2019**, *8*, 101.
[122] Z. Li, G. Geng, J. Cheng, W. Liu, S. Yu, B. Xie, H. Cheng, J. Li, W. Zhou, J. Tian, S. Chen, *Adv. Opt. Mater.* **2022**, *10*, 2200185.
[123] Z. Li, W. Liu, H. Cheng, S. Chen, J. Tian, *Sci. Rep.* **2017**, *7*, 8204.
[124] J. Cheng, Z. Li, D. Y. Choi, S. Yu, W. Liu, H. Wang, Y. Zhang, H. Cheng, J. Tian, S. Chen, *Adv. Opt. Mater.* **2022**, *10*, 2202329.
[125] R. Fu, K. Chen, Z. Li, S. Yu, G. Zheng, *Opto-Electron. Sci.* **2022**, *1*, 220011.
[126] F. Yue, C. Zhang, X. F. Zang, D. Wen, B. D. Gerardot, S. Zhang, X. Chen, *Light: Sci. Appl.* **2018**, *7*, 17129.
[127] J. Deng, Z. Li, J. Li, Z. Zhou, F. Gao, C. Qiu, B. Yan, *Adv. Opt. Mater.* **2022**, *10*, 2200949.
[128] Z. Li, W. Liu, H. Cheng, D. Y. Choi, S. Chen, J. Tian, *Adv. Opt. Mater.* **2019**, *7*, 1900260.
[129] B. Yang, H. Cheng, S. Chen, J. Tian, *Mater. Chem. Front.* **2019**, *3*, 750.
[130] V. Flauraud, M. Reyes, R. Paniagua-Domínguez, A. I. Kuznetsov, J. Brugger, *ACS Photonics* **2017**, *4*, 1913.
[131] S. Sun, Z. Zhou, C. Zhang, Y. Gao, Z. Duan, S. Xiao, Q. Song, *ACS Nano* **2017**, *11*, 4445.
[132] W. Yang, S. Xiao, Q. Song, Y. Liu, Y. Wu, S. Wang, J. Yu, J. Han, D. P. Tsai, *Nat. Commun.* **2020**, *11*, 1864.
[133] Z. Yang, Y. Chen, Y. Zhou, Y. Wang, P. Dai, X. Zhu, H. Duan, *Adv. Opt. Mater.* **2017**, *5*, 1700029.
[134] K. T. Lee, S. Y. Han, H. J. Park, *Adv. Opt. Mater.* **2017**, *5*, 1700284.
[135] J. Jang, T. Badloe, Y. Yang, T. Lee, J. Mun, J. Rho, *ACS Nano* **2020**, *14*, 15317.
[136] B. Yang, W. Liu, D. Y. Choi, Z. Li, H. Cheng, J. Tian, S. Chen, *Adv. Opt. Mater.* **2021**, *9*, 2100895.
[137] H. Wang, Q. Ruan, H. Wang, S. D. Rezaei, K. T. Lim, H. Liu, W. Zhang, J. Trisno, J. Y. E. Chan, J. K. Yang, *Nano Lett.* **2021**, *21*, 4721.
[138] C. U. Hail, G. Schnoering, M. Damak, D. Poulikakos, H. Eghlidi, *ACS Nano* **2020**, *14*, 1783.
[139] S. Yu, J. Cheng, Z. Li, W. Liu, H. Cheng, J. Tian, S. Chen, *ChemPhysMater* **2022**, *1*, 6.
[140] B. Yang, W. Liu, Z. Li, H. Cheng, S. Chen, J. Tian, *Adv. Opt. Mater.* **2018**, *6*, 1701009.
[141] H. L. Liu, B. Zhang, T. Gao, X. Wu, F. Cui, W. Xu, *Nanoscale* **2019**, *11*, 5506.
[142] B. Yang, D. Ma, W. Liu, D. Y. Choi, Z. Li, H. Cheng, J. Tian, S. Chen, *Optica* **2022**, *9*, 217.
[143] L. Gao, X. Li, D. Liu, L. Wang, Z. Yu, *Adv. Mater.* **2019**, *31*, 1905467.
[144] Z. Dong, L. Jin, S. D. Rezaei, H. Wang, Y. Chen, F. Tjiptoharsono, J. Ho, S. Gorelik, R. J. H. Ne, Q. Ruan, C.-W. Qiu, J. K. Yang, *Sci. Adv.* **2022**, *8*, eabm4512.
[145] K. Yang, M. Pu, X. Li, X. Ma, J. Luo, H. Gao, X. Luo, *Nanoscale* **2016**, *8*, 12267.
[146] Y. Hu, X. Luo, Y. Chen, Q. Liu, X. Li, Y. Wang, N. Liu, H. Duan, *Light: Sci. Appl.* **2019**, *8*, 86.
[147] Z. Li, M. Premaratne, W. Zhu, *Nanophotonics* **2020**, *9*, 3687.
[148] B. Wang, F. Dong, Q. T. Li, D. Yang, C. Sun, J. Chen, Z. Song, L. Xu, W. Chu, Y.-F. Xiao, Q. Gong, Y. Li, *Nano Lett.* **2016**, *16*, 5235.
[149] Y. Shi, C. Wan, C. Dai, Z. Wang, S. Wan, G. Zheng, S. Zhang, Z. Li, *Laser Photonics Rev.* **2022**, *16*, 2100638.
[150] B. Wang, F. Dong, D. Yang, Z. Song, L. Xu, W. Chu, Q. Gong, Y. Li, *Optica* **2017**, *4*, 1368.
[151] L. Deng, J. Deng, Z. Guan, J. Tao, Y. Chen, Y. Yang, D. Zhang, J. Tang, Z. Li, Z. Li, S. Yu, G. Zheng, H. Xu, C.-W. Qiu, S. Zhang, *Light: Sci. Appl.* **2020**, *9*, 101.
[152] Q. Dai, Z. Guan, S. Chang, L. Deng, J. Tao, Z. Li, S. Yu, G. Zheng, S. Zhang, *Adv. Funct. Mater.* **2020**, *30*, 2003990.
[153] R. Ren, Z. Li, L. Deng, X. Shan, Q. Dai, Z. Guan, G. Zheng, S. Yu, *Nanophotonics* **2021**, *10*, 2903.
[154] Z. Li, W. Liu, H. Cheng, S. Chen, *Sci. China: Phys., Mech. Astron.* **2020**, *63*, 284202.
[155] A. Forouzmand, H. Mosallaei, *ACS Photonics* **2018**, *5*, 1427.
[156] Y. Zhou, I. I. Kravchenko, H. Wang, H. Zheng, G. Gu, J. Valentine, *Light: Sci. Appl.* **2019**, *8*, 80.
[157] H. X. Xu, G. Hu, M. Jiang, S. Tang, Y. Wang, C. Wang, Y. Huang, X. Ling, H. Liu, J. Zhou, *Adv. Mater.* **2019**, *5*, 1900710.
[158] R. Xie, G. Zhai, X. Wang, D. Zhang, L. Si, H. Zhang, J. Ding, *Adv. Opt. Mater.* **2019**, *7*, 1900594.
[159] W. Ma, Z. Liu, Z. A. Kudyshev, A. Boltasseva, W. Cai, Y. Liu, *Nat. Photonics* **2021**, *15*, 77.
[160] Z. Li, W. Liu, D. Ma, S. Yu, H. Cheng, D. Y. Choi, J. Tian, S. Chen, *Phys. Rev. Appl.* **2022**, *17*, 024008.
[161] G. Li, S. Zhang, T. Zentgraf, *Nat. Rev. Mater.* **2017**, *2*, 17010.
[162] Z. Li, W. Liu, Z. Li, C. Tang, H. Cheng, J. Li, X. Chen, S. Chen, J. Tian, *Laser Photonics Rev.* **2018**, *12*, 1800164.
[163] M. Qiu, M. Jia, S. Ma, S. Sun, Q. He, L. Zhou, *Phys. Rev. Appl.* **2018**, *9*, 054050.
[164] X. Zhang, Q. Li, F. Liu, M. Qiu, S. Sun, Q. He, L. Zhou, *Light: Sci. Appl.* **2020**, *9*, 76.
[165] A. Caillas, S. Suffit, P. Filloux, E. Lhuillier, A. Degiron, *Nano Lett.* **2022**, *22*, 2155.
[166] X. Wang, A. Díaz-Rubio, V. S. Asadchy, G. Ptitcyn, A. A. Generalov, J. Ala-Laurinaho, S. A. Tretyakov, *Phys. Rev. Lett.* **2018**, *121*, 256802.
[167] Y. Bao, Y. Yu, H. Xu, Q. Lin, Y. Wang, J. Li, Z.-K. Zhou, X. H. Wang, *Adv. Funct. Mater.* **2018**, *28*, 1805306.
[168] F. Zangeneh-Nejad, D. L. Sounas, A. Alù, R. Fleury, *Nat. Rev. Mater.* **2021**, *6*, 207.
[169] Y. Zhou, H. Zheng, I. I. Kravchenko, J. Valentine, *Nat. Photonics* **2020**, *14*, 316.
[170] H. Kwon, A. Cordaro, D. Sounas, A. Polman, A. Alù, *ACS Photonics* **2020**, *7*, 1799.
[171] O. Reshef, M. P. DelMastro, K. K. Bearne, A. H. Alhulaymi, L. Giner, R. W. Boyd, J. S. Lundeen, *Nat. Commun.* **2021**, *12*, 3512.

[172] W. Ye, Y. Gao, J. Liu, *Phys. Rev. Lett.* **2020**, *124*, 153904.
[173] B. Wang, W. Liu, M. Zhao, J. Wang, Y. Zhang, A. Chen, F. Guan, X. Liu, L. Shi, J. Zi, *Nat. Photonics* **2020**, *14*, 623.
[174] X. Yin, J. Jin, M. Soljačić, C. Peng, B. Zhen, *Nature* **2020**, *580*, 467.
[175] Y. Zeng, G. Hu, K. Liu, Z. Tang, C. W. Qiu, *Phys. Rev. Lett.* **2021**, *127*, 176101.
[176] M. Wu, L. Ding, R. P. Sabatini, L. K. Sagar, G. Bappi, R. Paniagua-Domínguez, E. H. Sargent, A. I. Kuznetsov, *Nano Lett.* **2021**, *21*, 9754.
[177] M. Piccardo, M. de Oliveira, A. Toma, V. Aglieri, A. Forbes, A. Ambrosio, *Nat. Photonics* **2022**, *16*, 359.
[178] X. Zhang, Y. Liu, J. Han, Y. Kivshar, Q. Song, *Science* **2022**, *377*, 1215.
[179] W. T. Chen, A. Y. Zhu, F. Capasso, *Nat. Rev. Mater.* **2020**, *5*, 604.
[180] P. Georgi, M. Massaro, K. H. Luo, B. Sain, N. Montaut, H. Herrmann, T. Weiss, G. Li, C. Silberhorn, T. Zentgraf, *Light: Sci. Appl.* **2019**, *8*, 70.
[181] Y. Qu, S. Yi, L. Yang, Z. Yu, *Appl. Phys. Lett.* **2022**, *121*, 040501.
[182] H. Altug, S. H. Oh, S. A. Maier, J. Homola, *Nat. Nanotechnol.* **2022**, *17*, 5.
[183] J. Xiong, X. Cai, K. Cui, Y. Huang, J. Yang, H. Zhu, W. Li, B. Hong, S. Rao, Z. Zheng, S. Xu, Y. He, F. Liu, X. Feng, W. Zhang, *Optica* **2022**, *9*, 461.
[184] A. Ji, J. H. Song, Q. Li, F. Xu, C. T. Tsai, R. C. Tiberio, B. Cui, P. Lalanne, P. G. Kik, D. A. B. Miller, M. L. Brongersma, *Nat. Commun.* **2022**, *13*, 7848.
[185] X. Zhang, S. Yang, W. Yue, Q. Xu, C. Tian, X. Zhang, E. Plum, S. Zhang, J. Han, W. Zhang, *Optica* **2019**, *6*, 1190.
[186] S. Yi, J. Xiang, M. Zhou, Z. Wu, L. Yang, Z. Yu, *Nat. Commun.* **2021**, *12*, 6002.
[187] Y. Guo, S. Zhang, M. Pu, Q. He, J. Jin, M. Xu, Y. Zhang, P. Gao, X. Luo, *Light: Sci. Appl.* **2021**, *10*, 63.
[188] B. Fang, Z. Wang, S. Gao, S. Zhu, T. Li, *Nanophotonics* **2022**, *11*, 1923.
[189] H. Sroor, Y. W. Huang, B. Sephton, D. Naidoo, A. Vallés, V. Ginis, C.-W. Qiu, A. Ambrosio, F. Capasso, A. Forbes, *Nat. Photonics* **2020**, *14*, 498.
[190] S. Kruk, Y. Kivshar, *ACS Photonics* **2017**, *4*, 2638.
[191] T. Gu, H. J. Kim, C. Rivero-Baleine, J. Hu, *Nat. Photonics* **2023**, *17*, 48.
[192] X. Guo, Y. Ding, Y. Duan, X. Ni, *Light: Sci. Appl.* **2019**, *8*, 123.
[193] Q. Ma, G. D. Bai, H. B. Jing, C. Yang, L. Li, T. J. Cui, *Light: Sci. Appl.* **2019**, *8*, 98.
[194] E. B. Whiting, S. D. Campbell, L. Kang, D. H. Werner, *Opt. Express* **2020**, *28*, 24229.
[195] C. Wan, Q. Cao, J. Chen, A. Chong, Q. Zhan, *Nat. Photonics* **2022**, *16*, 519.
[196] A. Chong, C. Wan, J. Chen, Q. Zhan, *Nat. Photonics* **2020**, *14*, 350.
[197] A. H. Dorrah, N. A. Rubin, A. Zaidi, M. Tamagnone, F. Capasso, *Nat. Photonics* **2021**, *15*, 287.
[198] A. H. Dorrah, N. A. Rubin, M. Tamagnone, A. Zaidi, F. Capasso, *Nat. Commun.* **2021**, *12*, 6249.
[199] C. Zheng, J. Li, J. Liu, J. Li, Z. Yue, H. Li, F. Yang, Y. Zhang, Y. Zhang, J. Yao, *Laser Photonics Rev.* **2022**, *16*, 2200236.
[200] Q. Wang, E. T. Rogers, B. Gholipour, C. M. Wang, G. Yuan, J. Teng, N. I. Zheludev, *Nat. Photonics* **2015**, *10*, 60.
[201] A. Lininger, A. Y. Zhu, J. S. Park, G. Palermo, S. Chatterjee, J. Boyd, F. Capasso, G. Strangi, *Proc. Natl. Acad. Sci. U. S. A.* **2020**, *117*, 20390.
[202] E. Arbabi, A. Arbabi, S. M. Kamali, Y. Horie, M. Faraji-Dana, A. Faraon, *Nat. Commun.* **2018**, *9*, 812.
[203] L. Li, T. J. Cui, W. Ji, S. Liu, J. Ding, X. Wan, Y. B. Li, M. Jiang, C.-W. Qiu, S. Zhang, *Nat. Commun.* **2017**, *8*, 197.
[204] A. M. Shaltout, K. G. Lagoudakis, J. van de Groep, S. J. Kim, J. Vučković, V. M. Shalaev, M. L. Brongersma, *Science* **2019**, *365*, 374.
[205] Z. Lin, Y. Lin, H. Li, M. Xu, M. He, W. Ke, H. Tan, Y. Han, Z. Li, D. Wang, X. S. Yao, S. Fu, S. Yu, X. Cai, *Light: Sci. Appl.* **2022**, *11*, 93.
[206] P. R. Wiecha, A. Arbouet, C. Girard, O. L. Muskens, *Photonics Res.* **2021**, *9*, B182.
[207] Z. Liu, D. Zhu, L. Raju, W. Cai, *Adv. Sci.* **2021**, *8*, 2002923.
[208] Z. Li, R. Pestourie, Z. Lin, S. G. Johnson, F. Capasso, *ACS Photonics* **2022**, *9*, 2178.
[209] M. M. Elsawy, S. Lanteri, R. Duvigneau, J. A. Fan, P. Genevet, *Laser Photonics Rev.* **2020**, *14*, 1900445.
[210] S. Zhang, *Light: Sci. Appl.* **2022**, *11*, 242.
[211] N. Bonod, S. Bidault, G. W. Burr, M. Mivelle, *Adv. Opt. Mater.* **2019**, *7*, 1900121.
[212] R. Iten, T. Metger, H. Wilming, L. Del Rio, R. Renner, *Phys. Rev. Lett.* **2020**, *124*, 010508.
[213] G. Genty, L. Salmela, J. M. Dudley, D. Brunner, A. Kokhanovskiy, S. Kobtsev, S. K. Turitsyn, *Nat. Photonics* **2020**, *15*, 91.
[214] Z. Liu, D. Zhu, S. P. Rodrigues, K. T. Lee, W. Cai, *Nano Lett.* **2018**, *18*, 6570.
[215] L. Li, H. Ruan, C. Liu, Y. Li, Y. Shuang, A. Alù, C.-W. Qiu, T. J. Cui, *Nat. Commun.* **2019**, *10*, 1082.
[216] C. Liu, Q. Ma, Z. J. Luo, Q. R. Hong, Q. Xiao, H. C. Zhang, L. Miao, W. M. Yu, Q. Cheng, L. Li, T. J. Cui, *Nat. Electron.* **2022**, *5*, 113.
[217] H. Pinkard, Z. Phillips, A. Babakhani, D. A. Fletcher, L. Waller, *Optica* **2019**, *6*, 794.

Wenwei Liu is a research associate at the School of Physics, Nankai University. He received his Ph.D. degree in Physics from the Key Laboratory of Weak Light Nonlinear Photonics, Ministry of Education, Nankai University, China. His current research interests are high-Q photonics, imaging nanophotonics, and multifunctional integration based on metamaterials and metasurfaces.

Zhancheng Li is a research associate at the School of Physics, Nankai University, China. He received his Ph.D. degree in Optics from Nankai University in 2018. His research interests include chiral nanophotonics and multidimensional manipulation of optical waves based on metasurfaces.

Muhammad Afnan Ansari is a postdoctoral researcher in the Experimental Nanophotonics Group at Heriot-Watt University, UK. He received a Ph.D. degree in Electrical Engineering with a specialization in Flat Optics and Metasurfaces in 2021. His research interests include the fundamental physics of metasurfaces and its applications in ultrathin optical devices for holography, microscopy, and polarization detection. Under the research fellowship program for international researchers, he was awarded a prestigious fellowship by the Scientific and Technological Research Council of Turkey (TÜBİTAK) in 2018.